THESIS FOR THE DEGREE OF DOCTOR OF PHILOSOPHY

Critical Aspects of Delubrication and Sintering of Chromium-alloyed Powder Metallurgy Steels

Seshendra Karamchedu

Critical Aspects of Delubrication and Sintering of Chromium-alloyed Powder Metallurgy Steels

SESHENDRA KARAMCHEDU

Department of Materials and Manufacturing Technology

Chalmers University of Technology

SE-412 96 Gothenburg

Sweden

Telephone + 46 (0)31-772 1000

Critical Aspects of Delubrication and Sintering of Chromium-alloyed Powder Metallurgy Steels

Seshendra Karamchedu

Abstract

The cost efficiency and performance of Powder Metallurgy (PM) steels can be improved by replacing conventionally used alloying elements such as copper and nickel with chromium. Utilizing chromium imposes a challenge in terms of processing due to its effect on powder compressibility and high oxygen affinity, the latter of which, to a certain extent, is dealt with by introducing chromium in prealloyed form that decreases its activity. Therefore, each stage in the PM processing route has to be reconsidered to satisfy the thermodynamic and kinetic requirements to appropriately sinter components based on chromium alloyed steel powder for manufacturing high-performance PM parts. For conventional PM steels, consolidation is typically achieved by compaction, where the final dimensions of the part are achieved, followed by sintering, where metallurgical bonding between the powder particles takes place.

To facilitate compaction, powder is mixed with lubricant, which also improves the tool life; but the lubricant has to be removed prior to sintering. Among the problems encountered during sintering, those concerning delubrication are frequent but are difficult to detect. In the present study, a reliable approach for in-situ monitoring of the delubrication of PM steel compacts is presented. The method is based on continuous monitoring of the process atmosphere using sensors commonly used in the industry (CO_2 and O_2). Using this method, the effect of various process parameters on lubricant removal has been investigated and the changes occurring in the surface chemistry of the compacts during delubrication and their impact on sintering have been assessed. Based on these studies, delubrication at 450 °C in dry N_2 with dynamic gas flow conditions around the sample and a low heating rate were proposed to be optimum for the delubrication of chromium-alloyed PM steels.

Sintering of water-atomized chromium-alloyed powder compacts is typically performed in hydrogen-containing atmospheres with nitrogen as the carrier gas. However, attaining good carbon control in these atmospheres is challenging. Hence, the effect of different active constituents in the atmosphere, such as hydrogen, carbon monoxide and propane, on the reduction-oxidation and carburization-decarburization processes during the sintering of chromium-alloyed PM steels was investigated. It was shown that concentration of carbon monoxide above 1 vol.% in the sintering atmosphere results in significant oxidation of the compacts, whereas lower concentrations contribute to counteract the carbon loss and provide for the possibility of carburization during a continuous sintering process. Furthermore, lean atmospheres containing carbon monoxide, hydrogen and hydrocarbons as active constituents, with their total concentration not exceeding 5 vol. %, were shown to be potential candidates for sintering of chromium-alloyed PM steels, since they provide carburization while confining oxidation to acceptable levels.

Key words: chromium-alloyed sintered steels, delubrication, surface oxide, oxide reduction, sintering atmosphere, carbon control

Preface

This PhD thesis is based on the work performed at the Department of Materials and Manufacturing Technology, Chalmers University of Technology, between November 2010 and August 2015. The project work has been carried out under the supervision of Associate Professor Eduard Hryha and Professor Lars Nyborg.

This thesis consists of an introductory part with emphasis on aspects relating to delubrication and sintering of PM steels and a summary of the work performed which is included in the following appended papers:

I. Delubrication of PM components based on Cr-prealloyed steel powder - chances and risks

E. Hryha, S. Karamchedu, L. Nyborg

Proceedings of Euro PM 2011, 2011, Vol.3, pp.105-110

II. Influence of process parameters on the delubrication of PM steels

S. Karamchedu, E. Hryha, L. Nyborg

Powder Metallurgy Progress, 2011, Vol. 11(1), pp.90-96

III. Control of delubrication process for PM components based on prealloyed steel powders

E. Hryha, S. Karamchedu, L. Nyborg

Proceedings of the 2012 Powder Metallurgy World Congress & Exhibition, Japan Powder Metallurgy Association and Japan Society of Powder and Powder Metallurgy (2013), 15C-T2-10 (CD-ROM), ISBN: 978-4-9900214-9-8.

IV. Changes in the surface chemistry of chromium-alloyed powder metallurgical steel during delubrication and their impact on sintering

S. Karamchedu, E. Hryha, L. Nyborg

Journal of Materials Processing Technology, 2015, Volume 223, pp.171-185

V. Effect of active components of sintering atmosphere on reduction/oxidation processes during sintering of Cr-alloyed PM steels

E. Hryha, S. Karamchedu, D. Riabov, L. Nyborg, S. Berg

Journal of the American Ceramic Society, 2015, DOI: 10.1111/jace.13607

VI. Lean atmospheres for sintering of chromium alloyed powder metallurgy steels

S. Karamchedu, E. Hryha, L. Nyborg

Journal of the American Ceramic Society, 2015, DOI: 10.1111/jace.13617

VII. Effect of reducing agents in the atmosphere on the sintering of chromium alloyed PM steels

S. Karamchedu, E. Hryha, L. Nyborg

Manuscript

Contribution to the appended papers

   I.   Part of the experimental work was performed by the author.
  II.   The author planned and executed the experimental work. The paper was written mainly by the author in cooperation with the co-authors.
 III.   The author participated in the planning of the work, has performed a part of the experimental work and participated in writing the paper.
  IV.   The author performed the delubrication and sintering experiments and the SEM and EDS analysis on the fracture surfaces. The author participated in the XPS characterization and evaluated the results. The paper was written mainly by the author in cooperation with the co-authors.
   V.   The author participated in the planning of the work, has performed a part of the experimental work and participated in the presentation of the paper.
  VI.   The author planned and executed the experimental as well as the analytical work. The paper was written mainly by the author in cooperation with the co-authors.
 VII.   The author planned and executed the experimental work. The manuscript was written mainly by the author in cooperation with the co-authors.

Papers not appended to this thesis

    i.   Influence of delubrication process on the properties of sintered PM components

   S. Karamchedu, E. Hryha, L. Nyborg

   Proceedings of Euro PM 2013, Gothenburg, Sweden, Vol.2, pp. 163-168

Note: Results from this work were included in the expanded Paper IV, appended to the thesis.

   ii.   Lean atmospheres for sintering chromium alloyed PM steels

   S. Karamchedu, E. Hryha, S. Berg, S. Wiberg, L. Nyborg

   Proceedings of Euro PM 2013, Gothenburg, Sweden, Vol.2, pp. 353-358

Note: Results from this work were included in the expanded Paper V, appended to the thesis.

  iii.   Sinter-hardening response of sintered steel based on Astaloy Mo and its diffusion bonded derivatives

   S. Karamchedu, S. Hatami, L. Nyborg, M. Andersson

   Powder Metallurgy Progress, Vol. 14 (2), pp.93-98

Note: The work presented in this paper was useful for understanding the microstructural aspects concerning sinter-hardening of widely used diffusion bonded PM steel powders, for which, Cr-alloyed PM steels studied in this thesis can be a potential replacement.

Contents

1 BACKGROUND

Powder metallurgy (PM) steels for structural components are typically produced from water-atomized powder that is consolidated through uniaxial compaction followed by sintering. In such a process, the final dimensions of the part are already achieved after the compaction stage and the dimensional changes occurring during sintering are minimal. The subsequent sintering operation imparts bonding between the particles in the form of 'sinter-necks' which provides the necessary strength to the compacts [1]. Achievement of near net-shape with relatively few processing steps along with high material utilization and low energy consumption provides a competitive edge for the PM technology. It is known that improving mechanical performance of the parts is necessary to ensure market growth and maintain competitiveness with other production techniques. Among other approaches, this is being addressed through the development of cost-effective alloy systems suitable for high performance applications. In this context, water atomized chromium-prealloyed powder was developed as a cost and performance efficient alternative to replace the conventional PM steel powders alloyed with Cu, Mo and Ni [2]. Utilizing chromium as an alloying element, however, requires that each step in the manufacturing process is redefined to deal with the high oxygen sensitivity of chromium, particularly sintering.

Sintering is usually performed in continuous furnaces at elevated temperatures under protective gas atmospheres. Prior to compaction the powder is mixed with additives. These additives include lubricants which reduce the inter-particle friction and the friction between the powder and the die-wall during pressing. After compaction, lubricants have to be removed since they pose problems during the subsequent sintering stages. This is usually achieved in the initial zone of the sintering furnaces through thermolysis. However, problems concerning lubricant removal are frequently encountered industrially and hence a carefully controlled lubricant removal process is vital [3]–[7]. Improper delubrication can result in the deposition of lubricant decomposition products on the furnace parts and compacts, or in defects such as sooting and micro-cracking of the compacts which decrease the yield and increase maintenance costs. Previous studies concerning delubrication have attempted to optimize the parameters for efficient lubricant removal, based on which process control strategies were established. However, different opinions exist regarding the choice of time, temperature and particularly process atmosphere composition and it's purity to be employed for delubrication. Although complete lubricant removal can be easily obtained at a lab-scale, due to the complexity of the process it is relevant to obtain information on the lubricant removal in real-time in an industrial process. It has been suggested that monitoring of the processing gas composition would provide robust monitoring of the delubrication process [7]–[9].

The surface area of the powder compacts can be five orders of magnitude higher compared to their solid counterparts and hence play an important role during the processing of materials through the PM route. Increased surface area has a direct effect on the reactivity of the compacts

and hence the reactions at the surface are critical and determining for the final properties of the parts. Water atomized chromium prealloyed powder is covered by a heterogeneous oxide layer, consisting of a continuous layer of Fe-oxide – 6 to 8 nm in thickness and covering ~95% of the surface along with particulate oxide features rich in Cr and Mn of the size of a few hundred nanometers covering the rest of the surface [10], [11]. During sintering, the surface oxides have to be at least partially removed in order to facilitate the metallurgical bond formation between the powder particles, which imparts the required strength for the compacts. It can be inferred from the surface state of the chromium prealloyed powder that most of the particle contacts in the compact would be at the easily reducible Fe-oxide interfaces suggesting good sinterability of the powder.

From a delubrication point of view, it is important that the lubricant removal is performed in such a way that the surface chemistry of the compact is not negatively affected. Lubricants are complex organic compounds and during their decomposition the evolution of a number of gaseous constituents including CO_2, CO and heavy hydrocarbons was observed [12]. Of these, the presence of CO_2 in the sintering zone is especially critical as it can result in the oxidation of the powder by affecting the gas phase equilibria, which determine the efficiency of reduction of the oxides during sintering.

Graphite is added to the powder mix prior to compaction (along with the lubricant), which serves both as an alloying element and as a reducing agent during sintering. Apart from graphite, presence of hydrogen in the sintering atmosphere is considered advantageous since it aids the reduction of the Fe-oxide layer at low temperatures. Hence, water-atomized chromium-alloyed steel powder is typically sintered in hydrogen-containing atmospheres with nitrogen as the carrier gas. However, the presence of hydrogen in the sintering atmosphere can result in decarburization at elevated temperatures. Though the steel powder of interest exhibits high hardenability, a good carbon control during sintering would be necessary to utilize it and in order to make their processing robust. This is usually achieved by hydrocarbon additions. Although, problems with oxidation can be anticipated, carbon monoxide is another constituent that can possibly be used to obtain carbon control if utilized in appropriate concentrations and in combination with other active constituents in the sintering atmosphere. This approach, if proven beneficial in obtaining carburization in a continuous sintering operation, would contribute to a cost and performance efficient processing route for chromium-alloyed PM steels.

With regard to sintering of chromium-alloyed PM steels, the emphasis has hence been laid on: a) development of a method to monitor and study the delubrication process with industrial adaptability; b) study of the effect of delubrication on sintering with regards to the changes in surface chemistry imparted during delubrication; c) study of the oxidation/reduction and carburization/decarburization processes during the sintering in atmospheres containing carbon monoxide and d) assessment of the possibility and performance of sintering in lean atmospheres containing carbon monoxide, hydrogen and hydrocarbons as the active constituents.

2 POWDER METALLURGY

A brief overview of the powder metallurgy process is presented in this chapter. The correlation between various stages involved in the processing of powder metallurgy steels is discussed. This is to enable a better understanding of the issues concerning delubrication and sintering elaborated in chapters 3 and 4.

2.1 History and Outlook

The PM involves production and consolidation of metal powders into useful engineering components. A typical consolidation process consists of a forming stage where the powder is converted into the required shape (typically around room temperatures) followed by a temperature assisted sintering process which facilitates the formation of metallurgical bonds between the powder particles. The emergence and development of PM can be studied in connection with three principle characteristics of the process.

The first characteristic is that the process route *does not involve melting of the major constituent*. Making objects without melting is traced back to early civilizations where products including iron implements were produced as early as 3000 BC [1], [13], since the technology for obtaining high enough temperatures for melting these metals was not available. After the emergence of melting technologies, PM was largely ignored. The PM technology was revived for production of tungsten filaments for the same reason that tungsten could not be processed through the melting route. The second characteristic of PM is connected to the *usage of powder as the starting material*. This is advantageous in terms of upholding chemical homogeneity in the parts, as the segregation of the elements is restricted to the size of the powder. This also permits for freedom in alloy design since strict compositional control and otherwise unachievable compositions can be realized due to rapid solidification during powder production restricting the alloying elements to the solid solution. Based on this principle, products like tool steels and super alloys were developed. The third characteristic that is more relevant to PM steels and the context of this thesis is the *capability of the process to produce complex, net-shaped, high-quality precision components, while being suitable for high volume production*. This enables PM to compete with other manufacturing methods like casting, machining and forging while being cost efficient. The cost effectiveness of PM is because the process avoids or minimizes machining, allows maximum utilization of the raw materials (>95%), requires the lowest amount of energy per kilogram to produce a finished part and has a short overall production time [1], [14]. These factors contribute to the recognition of PM as a 'green technology' for sustainable manufacturing [15]. Sintered steel components have evolved on the basis of net-shaped high volume production capability of the PM process. Since then, developments have taken place more than for any other reason on the basis of the cost effectiveness of the process in this regard. The largest consumer for PM structural parts is the automotive industry. In a recent review it has been estimated that the average weight of PM parts per car is around 10 kg

for those manufactured in Europe and 19.8 kg for those manufactured in North America [16], [17].

2.2 Powder Metallurgy Steels

PM steels have become the most significant products of PM technology today and account for more than 80% of the total volume of all materials produced by this technique. Improvement in the quality of the powder, development of new alloy systems and sophistication in the processing techniques have extended the range of applications for sintered ferrous and ferrous alloy parts.

The PM process begins with the production of powder. To suit various applications, powder with a wide range of compositions, sizes, shapes and other attributes is produced using different manufacturing techniques. Several methods exist for the production of metal powder and can be broadly classified into (i) methods based on mechanical dispersion of solids and melts such as mechanical milling and atomization, and (ii) methods based on chemical processes such as solid-state reduction and electrolytic reduction. Overall, the production techniques employed for high volume and low cost production are water atomization and oxide reduction.

Iron or steel powder is generally mixed with lubricants, graphite powder and optionally other alloying elements (also in powder form) prior to the consolidation stage. The mixing process may also involve special treatments of the powder mix where organic binders are used to glue the additives to the iron/steel powder to improve the consistency and minimize segregation and 'dusting'.

Processing methods for PM steels can be categorized under pressure based densification, sintering based densification and hybrid densification methods [1]. In pressure based densification, the powder is compacted in a die where the final dimensions are set and minimum densification occurs during sintering [14]. For this case, the powders are large, compaction pressures are high and the sintering temperature is rather low. In contrast, for sintering-based densification the processing starts with loose powder, which is just shaped during the forming stage and then sintered to full or near full density at high temperatures. For such a process, powder size is small and sintering temperatures are high. Between these extremes are other processes, which rely on hybrid densification where the compaction and sintering stages are combined, like hot pressing and hot isostatic pressing. On a relative tonnage basis, press and sinter technology (pressure based densification) contributes to about 85-90% of the ferrous powder sales.

In the context of this thesis, powder production through atomization and pressure-based consolidation through uniaxial pressing and sintering are relevant and are discussed in the following sections.

4

Production of Iron and Steel Powders - Water Atomization
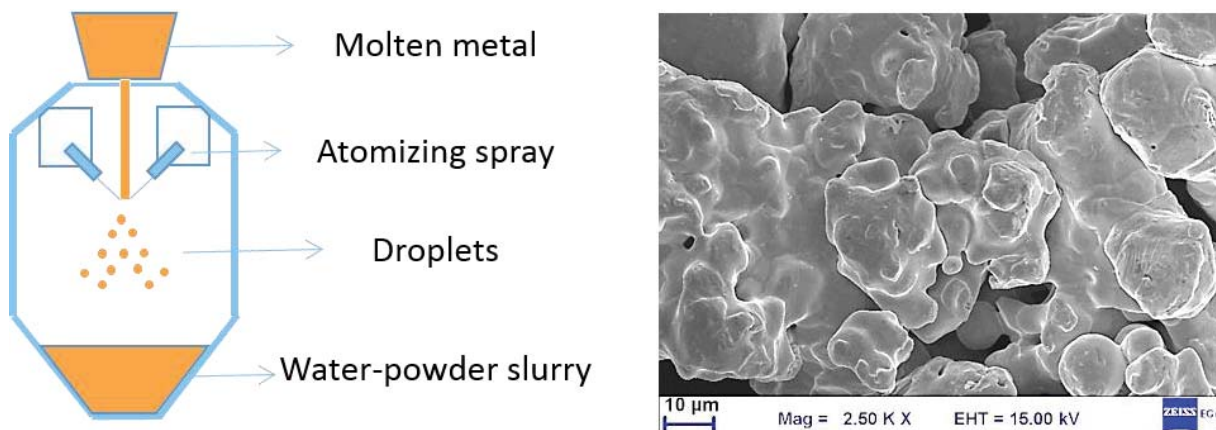
Figure 1 Schematic of the Water Atomization process (left) and SEM image of water atomized steel powder (right)

Water atomization is the predominant mode for production of elemental and ferrous alloy powder. In this process, molten metal is poured either directly or by means of a ladle into a tundish. The melt from the tundish runs down through a nozzle as a molten metal stream. High pressure water jets are directed onto the molten metal stream forcing it to disintegrate into droplets that solidify into powder (see Figure 1). The powder is obtained as a water-powder slurry which is subjected to drying to remove the water. Furthermore, water atomization results in irregular shape for the powder, as shown in Figure 1, which makes the powder suitable for compaction since this shape allows the metal particles to interlock during pressing. However, because of rapid cooling, the metal particles are hard (martensitic). They are also covered by oxide layers on the surface. The powder is hence subjected to drying, followed by a reduction annealing treatment to soften it and reduce the surface oxides. Thin iron-rich surface oxide products, typical for any metallic surface at ambient conditions, are observed on the powder surfaces after the reduction annealing due to their re-formation during cooling and handling [18]–[20]. The production rate by water atomization is very high which makes it suitable for high volume production at a rather low cost. The primary variable in this process is the pressure and geometry of the water jets and employing higher pressure results in finer powder sizes. The mean particle size used in practice is around 70-80 μm with 10-30% of the powder below 45 μm and less than 10% of the particles being above 150 μm [21]. Chemistry of the powder is another important variable. Alloying additions are usually added to the melt to atomize alloy powder. For water atomization, oxygen content of the powders is a good measure of the production quality. In general, high purity powder exhibits good compressibility and sinterability. Powder shape, size distribution and alloying content also affect compressibility.

Alloying

Ferrous powder is used mostly for structural applications and it has to be alloyed suitably to achieve the desired properties. In general, alloying elements decrease the compressibility of the powder and increase the cost. Steel powder can be classified into three different categories based on the method of alloying – *prealloyed, admixed* and *diffusion bonded* powders.

5

In prealloying, the alloying elements are added to the melt before water atomization, which results in a homogeneously alloyed powder. Another important advantage is that prealloying allows for the addition of oxidation sensitive alloying elements such as chromium and manganese, which are difficult to be introduced in other forms. The disadvantage with prealloying is that the compressibility of the powder is lowered as a possible consequence of the solid solution hardening effect of the alloying elements. Molybdenum is commonly used in prealloyed form due to its lower effect on compressibility. Molybdenum prealloyed grades are used as base powder for diffusion bonding and admixing.

In admixing, iron powder is mixed with alloying elements in the form of powder prior to the compaction stage. Alloying in this case is achieved during sintering through diffusion. The primary advantage of admixing is that the compressibility of the powder mix is high while the disadvantage is that it can result in inhomogeneous distribution of alloying elements due to their slow diffusion and segregation. Typically, carbon is added to ferrous powder in the admixed form as graphite since carbon has a highly detrimental effect on compressibility if prealloyed.

Diffusion bonding is a method where fine particles of the alloying element, typically of the size of a few tens of microns or lower, are bonded onto the surfaces of the iron powder through a diffusion-based annealing process. This again avoids segregation while retaining compressibility. However, inhomogeneity in distribution of alloying elements is still observed for the case of diffusion-bonded powders. Nickel and copper are usually alloyed by diffusion bonding to ferrous powder. An example showing the heterogeneity in the distribution of alloying elements in diffusion bonded powders can be seen in Figure 2 [22]. Regions rich in Ni can be observed since Ni was diffusion bonded while prealloyed Mo is uniformly distributed.

EDX	Fe	Ni	Mo
1	83.7	14,89	1,4
2	86,33	12,18	1,5
3	95,1	3,77	1,13
4	92,45	6,28	1,26
5	98,97	0	1,03
6	98,31	0	1,69
7	98,4	0	1,6
8	98,21	0,99	0,8
9	97,75	0,46	1,79
10	98,49	0	1,51
11	98,22	0	1,78
12	98,7	0	1,22
13	98,14	0,45	1,41
14	98,64	0	1,36
15	91,99	6,66	1,35
16	95,18	3,57	1,25
17	97,17	1,2	1,63
18	98,21	0	1,73
19	98,74	0	1,26
20	98,29	0	1,71
21	98,12	0,56	1,32
22	97,97	0,49	1,54
23	98,29	0	1,71
24	96,4	2,05	1,56
25	96,7	1,29	2,01

Iron Kα1   Nickel Kα1   Molybdenum Lα1

Martensitic   Bainitic-Martensitic   Ni- rich   Bainitic

Figure 2 SEM and EDS analysis of a powder prealloyed with Mo and diffusion bonded with Ni (from *Paper ii*)

Water-atomized steel powder, pre-alloyed with chromium and molybdenum, has been used in the present study.

Compaction - Uniaxial Pressing

In uniaxial pressing, the powder is placed inside a compaction tool and a compressive stress of 400-800 MPa is applied simultaneously from the top and bottom. Upon compaction, the metal particles interlock at the surface irregularities, and with increasing densification they plastically deform increasing the area of the particle contacts along with some degree of cold welding. The final mechanical properties of sintered parts are strongly dependent on the density values. Since the final shape of the part is already achieved after the compaction, it is an important stage, which dictates the density of the parts. Tensile strength and fatigue strength increase roughly linearly with increase in density [23]. The average density of the sintered parts has increased over the last few decades to meet the increasing performance demands. Achieving high density at relatively low cost by single press and single sintering is of prime importance for PM industry. Methods such as *warm compaction* - where the powder and the die are heated to around 150 °C, *warm die compaction* - where only the die is heated but not the powder and *high velocity compaction* - where the speed of compaction is increased up to 500 times, have been developed to improve the achievable density levels upwards by 0.2-0.3 g/cc [24]–[26]. Each of these methods has its own set of advantages and disadvantages. Since there is an increasing production cost associated with these processes, compaction at room temperature is still the most widely employed method for high volume industrial production.

Lubricants

Friction between the powder and die wall is a fundamental issue in traditional powder metallurgy involving die compaction. During pressing it has a major impact on the density gradients within the pressed part and during ejection, it influences the surface quality of the parts and causes tool wear. Lubricants are hence used to decrease the ejection forces and minimize the tool wear. Lubrication can be achieved either through admixed lubricants or die-wall lubrication. Typically, lubricants are admixed as fine particles to the metal powder in concentrations between 0.3 and 1.0 wt.% prior to compaction. Lubricants aid compaction by: a) reducing inter-particle friction which decreases the required compaction pressure and improves homogeneity of density distribution and b) reducing the friction between the powder and the die-wall which lowers the tool wear and heat buildup at the die-wall and improves the tool life. Hence, lubricants play an important role in the integrated approaches for achieving high densities [25].

Lubricants used for cold compaction can be divided into three groups: metal soaps, amides and composite lubricants. Metal soaps are the oldest group of solid lubricants used for compaction of metal powders. Zinc stearate is a popular lubricant, which falls under this category. The advantage with zinc stearate is that it provides good lubricity and flow properties for the powder mix. Its major disadvantages are environmental and health issues concerning zinc sublimation during the delubrication process and 'contaminating' removal often resulting in residues on the

surface of the compacts and on the furnace parts after delubrication [27]. The amides consist of di-amide with two fatty acid chains with stearic acid being the most common fatty acid chain used. Commercial amide waxes have a melting interval between 130 and 150 °C and can be efficiently delubricated [28] since they are purely organic. Common lubricant stearates contain 12 to 22 carbon atoms with a typical length of 18 carbon atoms and ethylene bis-stearamide (EBS, industrial name '*Acrawax*'), which is widely used for PM steels belongs to this family of lubricants. The disadvantage with amide waxes is their poorer flow properties compared to zinc stearate. Composite lubricants are complex organic compounds combining different chemical substances which provide possibilities to compose lubricants with properties tailored for specific applications [29]. Composite lubricants based on modified EBS are widely used as they provide superior or equivalent green and sintered properties as compared to pure EBS, especially with respect to the ejection forces [30]. It is a complicated process to select lubricants as their chemistry, powder size and shape all have conflicting implications. For example, finer lubricant particles are preferred for achieving higher densities while coarser particles are more effective in reducing the ejection forces. Powder mixes are specifically designed for warm compaction and warm die compaction since the lubricants should maintain lubricity even at increased temperatures [31].

Though lubricants aid compaction, several disadvantages such as reduction of powder flow rate, limitations on the compact green density and problems with improper delubrication are associated with them. Although indispensable for the reduction of die-wall friction and lowering of the ejection forces, lubricants possess also lowering effect on the achievable theoretical density levels for the powder mixes. During compaction, some part of the lubricant is squeezed towards the die-wall and only lubricant particles between the first powder layer and the tool wall participate in lubrication [32]. Rest of the lubricant gets entrapped inside the closed pores where it develops a hydraulic pressure opposing the densification process. In practice, the amount of lubricant is optimized, by striking a balance between the inter-particle friction, green strength, green density and ejection forces. Problems associated with lubricant removal are discussed in chapter 3.

Sintering

Compacts only possess modest strength (green strength) necessary for their handling after compaction and have to be sintered to impart the required mechanical performance for their application. During sintering, compacts are heated to high temperatures (2/3 to 4/5 of the melting temperature of the main component of the powder mix) to facilitate the formation of 'necks' between the particles. These inter-particle necks are formed at the particle contacts established during compaction and the neck formation is driven by the minimization of surface energy which progresses through atomic diffusion processes and evaporation/condensation mechanisms. A prerequisite for the sinter neck formation is sufficient reduction of the oxides present on the powder particle surfaces [33]–[35]. A typical sintering process consists of a heating phase, followed by a sintering phase where the compacts are held at a constant temperature for enough time to achieve sufficient bonding between the particles and finally a

cooling phase during which the microstructure is decided by the cooling rate as illustrated in Figure 3.

Before the beginning of sintering, the lubricant in the compact has to be removed so that it does not inhibit the neck formation between the particles. This is achieved through thermolysis during the initial stages of heating. For this purpose, a part of the furnace is kept at a controlled temperature, which is referred to as the delubrication/dewaxing/preheat zone.

Two features which are essential for performing sintering are furnaces and protective gas atmospheres. Two types of sintering furnaces are most commonly used industrially: batch and continuous furnaces. The advantage with batch furnaces is that individual processes such as delubrication and sintering can be optimized without interference between the process atmospheres. However, their productivity is lower when compared to continuous furnaces. Continuous furnaces on the other hand have high productivity and hence are used extensively for the production of PM parts. However, in continuous furnaces atmosphere optimization is difficult due to openings between the different zones.

Continuous furnaces are equipped with zones (chambers) for delubrication and pre-heating, sintering (high temperature) and cooling. Modern furnaces are equipped with fans in the cooling zone to perform accelerated cooling to harden the steel components directly after sintering thereby avoiding further heat treatment, which is referred to as sinter-hardening. Typical sintering temperatures for industrial production using continuous furnaces are in the 1120-1150 °C range and the holding time at this temperature is between 15 and 30 minutes. The maximum temperature limit is set by the strength of the mesh belt in relation to the stress caused by the load on the belt. Ceramic mesh belt, pusher or walking beam furnaces are used when sintering is to be performed at higher temperatures, up to 1250 °C. High temperature sintering is beneficial since more efficient sinter-neck formation and pore rounding due to accelerated diffusion processes and better reduction of oxides can be realized. Its disadvantage is that the dimensional control becomes more difficult, which is not desirable.
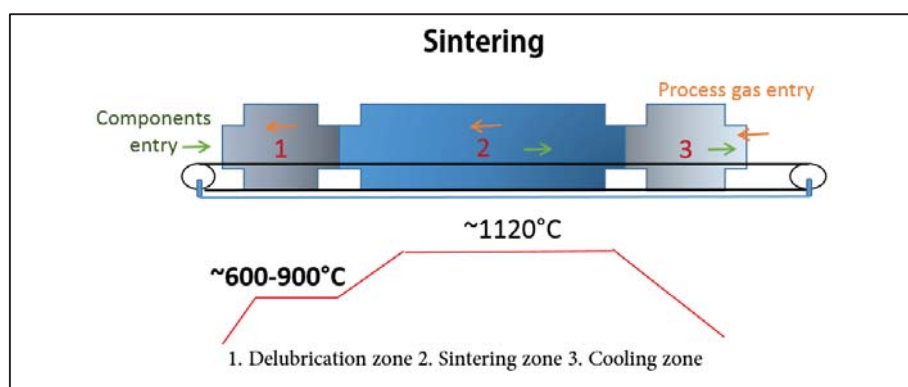
Figure 3 Schematic of a continuous sintering furnace

The second important feature for sintering is the protective atmospheres (term interchangeably used with sintering atmospheres/ process atmospheres/atmospheres/ processing gases), the primary purpose of which is to control the reactions between the compacts and surroundings.

Main functions that the sintering atmosphere have to ensure are: a) efficient removal of the delubrication products during preheating, b) reduction of surface oxides on the powder particles (or as minimum protecting powder surface from oxidation) to enable metal to metal contact, c) prevention of oxidation during sintering and cooling, and d) controlling the carbon content (carburization and decarburization reactions) of the ferrous parts. In order to flush out the lubricant decomposition and oxide reduction products out of the furnace and to prevent these products from entering the high temperature sintering zone, the flow of the sintering atmosphere is from the sintering zone to the delubrication zone. *Endogas* atmospheres produced through combustion of hydrocarbons are commonly used for sintering of ferrous components. However, for the case of steels containing oxidation sensitive alloying elements, like chromium, which is the case in the present study, high purity N_2 atmospheres containing up to 10 vol.% H_2 are used. Sometimes CH_4 or CO is added to the atmosphere to provide the possibility for carbon control during sintering. Aspects related to the influence of sintering atmosphere on the lubricant removal are discussed in chapter 3 and those concerning the compact-sintering atmosphere interactions are elaborated in chapter 4.

2.3 Chromium Alloyed PM Steels

Due to the high surface area present for the case of PM steels, they are subject to significant risk of oxidation compared to wrought steels. For this reason, traditionally, alloying elements such as Cu, Mo and Ni have been used as their oxides are easily reducible compared to that of Fe. Utilizing Cr as a substitute for these alloying elements provides several advantages. The first advantage is the economic benefit since Cu and Ni are significantly more expensive than Cr. Also, Ni is associated with health issues and Cu with recyclability problems. Furthermore, Cr provides a higher hardenability which makes it suitable for high performance applications [36] and sinter-hardening [37]. The major challenge concerning usage of Cr as an alloying element is its high oxygen affinity, which poses strict demands on processing. By prealloying, the activity of chromium can be reduced roughly down to its content. Also, it has been shown that for the low levels of chromium typically used, prealloying does not significantly degrade compressibility of the powders [38][39]. Though usage of chromium-alloyed powder has been demonstrated already in the eighties, such powder did not find extensive usage due to the expensive production methods [40]–[42]. Hence only about decade ago Höganäs AB, Sweden, introduced a cost-effective prealloyed steel powder grade Astaloy CrM containing 3 wt.% Cr and 0.5 wt.% Mo produced through water atomization and subsequent reduction annealing [2]. This powder grade is now well-established and used in production of PM steel parts for high performance applications. Delubrication and sintering studies in the present study have been conducted on compacts of this powder grade. Both Cr and Mo are ferrite stabilizers and the eutectoid carbon composition has been estimated to be around 0.4 wt.% using thermodynamic simulation software [43], [44], considering only the presence of austenite, ferrite and cementite and disregarding the presence of all equilibrium carbides based on the experimental investigation [45]. The eutectoid temperature is estimated to be around 775 °C which is in accordance with the well-established traditional empirical models [46].

3 DELUBRICATION

In this chapter, some critical aspects concerning delubrication are discussed with focus on EBS lubricants and previous research on this subject is reviewed. The main focus of the previous studies on delubrication has been to develop an approach for the determination of completion of the lubricant removal process.

3.1 Problems Associated with Delubrication

Several composite lubricants are used in the industry in accordance with varying requirements and hence delubrication of a wide range of products in the same furnace is challenging. While designing new lubricants, the ease with which they can be removed hence plays an important role [47]. Sooting, decrease in strength, variation in composition (particularly carbon), micro-cracking and variation in dimensions of the parts are defects resulting due to improper delubrication [3], [6], [48]. Some authors claim that EBS is prone to sooting since it has a hydrogen to carbon atomic ratio of 2 and does not decompose cleanly [7], [49]. Sooting is associated with one or a combination of the following factors: too low dew- point (i.e. water vapor content) in the preheat zone, too short holding times, too high belt speeds, too high belt loads, too high heating rates, cracking of hydrocarbons from the lubricant vapors or constituents in the sintering atmosphere. Some authors report that sooting need not necessarily be directly connected to the organic part of the lubricant [23] while others claim that sooting via lubricant vapors is plausible [7]. Sooting is observed in the form of stains, black spots, granular soot, internal sooting or blistering (which is the worst form of sooting) [3], [50]. Ingress of the lubricant vapors into the sintering zone can result in low strength and variation in carbon levels of the sintered compacts. This can also result from lubricant remaining in the compacts (resulting from incomplete delubrication) entering the high temperature sintering zone where it decomposes, deteriorating the purity of the sintering atmosphere (too high CO_2 or CO levels). Improper delubrication can also lead to deposition of delubrication products on the compacts and furnace parts, even in the cooling zone [51], leading to maintenance problems and increase in costs. The biggest risk in the case of powder alloyed with oxygen sensitive elements is the oxidation of the compacts during delubrication, either by the products of the lubricant decomposition or by the gaseous constituents in the delubrication zone, and hence has been the focus of this thesis.

3.2 Sequence of Events during Delubrication

Delubrication consists of two stages: melting and decomposition. Upon reaching the softening/melting point, lubricants melt and further decompose into a number of molecules including CO_2, CO, CH_4, C_2H_4, H_2O and heavy hydrocarbons [8], [9]. For EBS, the melting range is reported to be between 135 and 150 °C [7], [28], [52]. Decomposition depends on the chemical structure of the lubricant, and for EBS, it begins at temperatures as low as 150 °C with a maximum occurring around 450 °C [8]. The sequence of events identified through visual observation of the delubrication process is: melting of the lubricant, followed by the oozing out of the liquefied lubricant droplets to the surface of the compact where they coalesce into larger

droplets (see Figure 4) followed evaporation and disappearance of the lubricant droplets along with the formation of a semi-transparent dense gas [27], [53]. Also, some authors reported that bubbling of the lubricant was observed at some places on the compact surface prior to evaporation that was less prominent for EBS when compared to zinc stearate [27]. Oozing out of the molten lubricant is suggested to be due to the free-pore volume being insufficient to accommodate the molten lubricant [53]. It is also possible that the molten lubricant drips down from the bottom of the compact depending upon the density and geometry of the part [27], [54]. It is worth mentioning that the visual observations reported in the studies mentioned in this section were from delubrication experiments performed at high heating rates and hence the temperatures reported for the corresponding visual observation would vary with a change in heating rate. A detailed description of the results from visual examination of the delubrication process performed in the present research can be found in section 7.1. An example of the results obtained is shown in Figure 4, showing the formation and growth of lubricant droplets on the surface of the compact.

Figure 4 Images of the compact at different times during the delubrication process: visual observations from the present work

3.3 Chemistry of Delubrication

Determining the completion of the delubrication process requires a good understanding of how, and in which form the lubricant is removed, and what products are formed during this process. This information would be valuable for devising appropriate sensors for monitoring the delubrication process and is also crucial for the development of new lubricants. The chemical structure of the EBS molecules is shown in Figure 5.
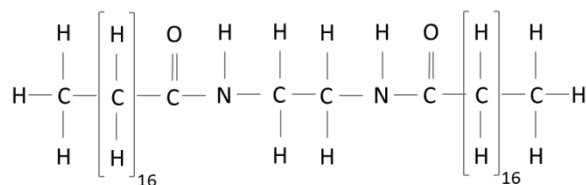
Figure 5 Chemical structure of the EBS molecule

Within the molecule, the bond strength varies between ~326 and ~544 kJ, indicating that the decomposition would be continual. In the ascending order of the bond strengths within the molecule, C-N bonds have the lowest value, followed by the C-C bonds at the center of the molecule, then C-C bonds at the extremes, followed by C-H bonds; C=O (double bonds) being

12

the strongest [7], [55]. In the previous studies where differential thermal analysis was performed on EBS, the authors report that it exhibits four endothermic peaks, three of which occur below 200 °C indicating melting, and a fourth endothermic peak related to decomposition occurs around 400 °C (heating rate was 10 °C/min) [7], [55].

Previous investigations where the gas-phase products produced during the thermolysis of EBS were studied revealed that CO_2 and aliphatic hydrocarbons with an absorption band between 3000 and 2700 cm^{-1} were the major emission products [8]. Their emissions were in tandem with maximum values around 450 °C and CO, CH_4, C_2H_4 and NH_3 were reported as the minor products. Also, the chemical structures of condensable large molecular hydrocarbons formed during the decomposition of EBS were identified. Based on these results, a reaction mechanism for lubricant pyrolysis was proposed. Similar results concerning the major delubrication products were observed in other studies [12], [56].

3.4 Effect of Process Parameters on Delubrication

There are conflicting opinions regarding the choice of process parameters for efficient delubrication which are discussed in this section. Industrial best practice to is to heat the compacts slowly below 600 °C, before they enter the high temperature zone to ensure complete lubricant removal [1]. However, temperatures up to 900 °C are used in practice [4].

Heating Rate

Heating rate has the most significant effect on delubrication according to a statistical study, suggesting that it is essentially a thermal process [57], [58]. It is reported that the temperature corresponding to lubricant removal shifts towards higher values with an increase in the heating rate [53], [57]–[59]. Some authors attribute this to the sluggish mass transfer rate compared to the high heat transfer rate; since mass transfer out of the compact involves processes such as melting, vaporization and decomposition which are slow [53].

According to some authors, slow heating rates are to be employed to ensure safe and complete lubricant removal [6], [55], [60]. The basis for this view is that, though the melting of the lubricant takes place around 150 °C, evaporation and progressive elimination only begins at higher temperatures, and most of the lubricant is removed in a narrow temperature interval between ~300 to less than 500 °C. It is hence argued that employing high heating rates in this temperature interval might result in rapid decomposition, and the associated volumetric changes might induce defects in the parts such as micro-cracking. This narrow temperature range for lubricant removal is suggested to be because of the relatively short carbon chain in EBS compared to other binders used, for example in metal injection mounding, such as polypropylene [49], [55], [60]. It is also believed that the presence of carbon containing vapors above 600 °C can lead to undesired reactions, such as sooting, which affects the final properties after sintering. Since higher heating rates shift delubrication to higher temperatures, the authors recommend a slow heating rate to minimize the effect of these undesired reactions. Contrary to this approach, it is argued that since the rate of sooting due to the decomposition of carbon monoxide and hydrocarbons in the atmospheres is high between 500-600 °C and is catalyzed

by the presence of metallic iron, nickel and cobalt, higher heating rates would avoid sooting as the compact passes through this regime quickly [53], [54], [61]–[63]. It is also claimed that higher heating rates might aid in breaking down the lubricant into smaller hydrocarbon species which can be flushed out easily [59].

Density and Sample Geometry

Density is expected to play a significant impact on delubrication since the mass transport of the molten lubricant and the lubricant vapors occurs through the pore channels of the compacts. However, for the compacts with relative densities between 85 to 94%, delubrication temperatures were found to be independent of the density [27], [59], [64]. In other studies, for compacts with densities below 90% of the relative density, an increase in the decomposition temperatures with an increase in density is reported [49], [65] and this increase is attributed to the dramatic decrease in the number of pores on the surface with the increase in density.

When densities exceed 7.0 g/cc, pores get almost filled with the lubricant and rapid heating under such circumstances can be expected to bring about a significant risk of defect formation in the compacts. Lubricant residues are also believed to be high in high density compacts due to the hindered transport of the lubricant [47]. Hence, for high density compacts, delubrication becomes much more critical. Generally, in the case of carbon deposition, for more porous compacts, internal carbon deposition is expected, while for high-density compacts, the deposition is supposed to be external [62].

In a study where lubricant removal in warm-compacted parts was studied, the beginning and ending of delubrication was reported to occur at lower temperatures compared to the cold-compacted ones [64]. This was attributed to the better metal-lubricant contact for the warm-compacted parts aiding heat transfer. Also, for the compacts subjected to warm compaction, the temperatures corresponding to the beginning and ending of delubrication were shown to decrease with an increase in the density of the compacts. The mass loss curves for lubricants used for warm compaction were different from those of the lubricants used for cold compaction due to their complex chemistry. However, the delubrication rate was found to be an intrinsic property of the lubricant, since for both room temperature and warm compaction, it was found to be independent of density [64].

Surface to volume ratio is considered to play a significant role on lubricant removal. However, experimental observations in some studies showed that there is little influence of the surface to volume ratio on the delubrication kinetics, indicating that the rate determining step for delubrication is the lubricant evaporation/decomposition [59]. This claim concedes with the visual observations of delubrication in another study [27]. For compacts with densities above 85% of the relative density, it is claimed that lower surface to volume ratio aids delubrication while the opposite is true for the case of the compacts with densities below the mentioned value [65].

14

Gas Flow Rates

Lubricant vapors drawn off with the furnace gas are removed at regular intervals, for which electrostatic separators are sometimes used [14]. When the gas flow in the furnace is insufficient, it can lead to condensation/deposition of the delubrication products on the furnace walls and compacts. When the amount of reactive gases in the atmosphere is low, meaning poor buffering capacity, imbalances caused due to the ingress of the lubricant decomposition products into the sintering zone is not taken care of, resulting in poor sintering. Moreover, insufficient gas flows can lead to soot deposition on the parts [6]. In a study related to the decomposition of Zn-stearate at high temperatures, it was observed that the gas- phase transfer plays a significant role [66]. When the gas flow was insufficient, it resulted in the formation of a stagnant lubricant vapor layer on the compact surface, increasing the local C to H concentration ratio above 1, leading to soot formation [66]. This principle is valid even for the pre-heat zone in the furnace where carbon-containing lubricant vapors are present. Although usually, continuous furnaces are used for sintering, in some cases, to prevent ingress of lubricant decomposition products into the high temperature sintering zone, furnaces with separated delubrication chambers which are connected at right angles, or furnaces with U-shaped construction are used [14].

Catalytic Effect

Based on the observations concerning the evolution of gas-phase products during the decomposition of EBS, it is proposed that lubricant removal is aided by the catalytic effect due to the iron/carbon matrix [67]. While in another investigation, it is reported that the catalytic effect due to iron/carbon matrix is minimum but the alloying elements can exercise this effect [12]. Furthermore, there are TG studies indicating that the effect of base powder on the delubrication process is insignificant [59], [64]. The extent to which the catalytic effects are active needs to be clarified.

Process Atmosphere

The presence and concentration of various gaseous constituents in the process atmosphere can alter the effectiveness of the delubrication process. Apart from flushing out the delubrication products, process atmosphere can play a role in the lubricant removal by providing reaction species, which aid decomposition of the organic molecules. The primary factor to be considered for the selection of process atmosphere for delubrication is the sensitivity of different materials with respect to it. For example, nitrogen-based atmospheres when used for stainless steels at high temperatures can result in nitrogen pickup. There are differing opinions regarding the choice of atmosphere for efficient delubrication- if it should be oxidizing, reducing, wet (high dew-point/moisture content) or dry (low dew-point). Studies supporting and opposing each view exist which are reviewed in the following sub-sections.

Neutral (dry): Delubrication performed in neutral dry atmospheres is advantageous in the sense that the atmosphere has little effect on the surface chemistry of the powder [1], [60], [68].

However, a popular notion is that the deficiency of hydrogen and oxygen in the lubricant leads to improper delubrication associated with the formation of soot when subjected to thermolysis in neutral-dry atmospheres. Development of lubricant mixes with additives consisting of oxidizing agents that oxidize the residues upon lubricant decomposition ensuring clean removal support this hypothesis [47]. Regarding neutral atmospheres, one view is that the usage of argon is effective in flushing out the heavy, long chained delubrication compounds, preventing their condensation on the cold parts of the furnace, since argon is heavy [69].

Oxygen/Air: Since lubricants do not possess enough oxygen molecules to decompose into CO and CO_2, which can be flushed out easily, it is argued that supplying sufficient oxygen improves breaking down of the hydrocarbon chains. For pure EBS, it was shown that the delubrication finish temperature (corresponding to 95% weight loss) decreased with the addition of 1 vol.% O_2 to the nitrogen gas [28]. However, with a further increase in the oxygen content, it increased and a maximum was reported for the case of delubrication in air. For the case of delubrication of stainless steel compacts, it was shown that it is effective to use air up to 400 °C, but above this temperature, a weight gain associated with oxidation of the powder was observed [68].

Burn-off units: Burn-off units are developed supporting the view of oxidizing atmospheres improving the delubrication efficiency. These units function based on injecting the off-gases produced upon igniting air and fuel mixtures of a given ratio using special burners to generate an oxidizing atmosphere. This ignition also generates heat. During burn-off, lubricant vapors along with the reducing atmosphere components such as carbon monoxide and hydrogen will be oxidized [70]. Lubricant burn-off is considered to be more effective than addition of oxygen to the process atmosphere [5], [69] and it is claimed that sooting can be avoided using the burn-off process [53], [62]. The biggest drawback with burn-off process is that it can cause oxidation of the compacts. The high heating rates employed during burn-off can also cause problems during delubrication, but at the same time, it is the most cost-effective way of heating up the compacts. There are also studies suggesting that burn-off gives varying and less repeatable properties of the compacts, especially with regard to oxidation of the components [1], [70].

Moisture: Among the oxidizing agents- oxygen, moisture and CO_2, some authors are of the opinion that addition of moisture to the process atmospheres is the most effective means for efficient lubricant removal since oxygen injected into the sintering atmosphere would nonetheless react to form water [4], [52], [58]. Higher dew-point is also considered to decrease the sooting tendency. Based on this, auxiliary systems such as bubblers and humidifiers for sintering furnaces have been introduced into the market [6]. A decrease in activation energy for lubricant decomposition in the presence of moisture is reported based on a kinetic model, suggesting that moisture plays a major role in the chemistry of decomposition [58]. It has been reported that moisture additions to argon improved the efficiency of delubrication and at the same time results in lower level of contamination in the material than when lubricant removal was performed in pure argon or argon mixed with air [69]. Although an improved efficiency in

16

delubrication was observed due to moisture addition, a weight gain during holding at the delubrication temperature corresponding to possible oxidation is reported [7]. There are also studies suggesting that humidity has a decreasing effect on the efficiency of delubrication [28], [68]. Further, in another investigation where the pyrolysis products of EBS decomposition were studied, the effect of moisture addition was observed to be minimum, except that the magnitude of CO peak observed above 800 °C doubled and shifted to higher temperatures in the presence of moisture [8].

The most common problem with devices used to introduce oxidizing constituents into the process atmosphere is related to the control of the amount of oxidant that is being introduced [6].

Hydrogen: From the experience of lubricant removal on steel strip coils, it is suggested that pure hydrogen gives the best results [71]. Some thermogravimetric studies on the delubrication of steel and stainless steel compacts support this claim [1], [7], [27], [68]. Since pure hydrogen is very expensive and unsafe, it is common practice to use nitrogen-hydrogen mixes. It was shown that higher hydrogen content provides greater weight loss of the lubricant [1]. Delubrication in N_2-H_2 yielded different pyrolysis gas-phase products compared to that in the case of pure N_2 [8]. In the presence of H_2, the CO peak observed at 725 °C for pure N_2 shifted to 850 °C along with a decrease in intensity. This can be due to the reduction of the surface oxides by hydrogen at lower temperatures [72]–[75].

There are approaches suggesting usage of a combination of the constituents mentioned above within the delubrication zone. For example, there are studies indicating that a combination of H_2 and H_2O with a high H_2/H_2O ratio gives the best delubrication results [1], [7], [28]. However, as discussed in the section 2.2, most of the industrial production for PM steel components takes place utilizing continuous sintering furnaces, where the control of sintering atmosphere in the different zones of the furnace is rather complicated, and in such cases, usually nitrogen-based atmospheres are used throughout the furnace.

3.5 Delubrication Monitoring Attempts

Most of the studies concerning delubrication have been performed based on utilizing thermogravimetric analysis for measuring the lubricant weight-loss under a specified time, temperature and atmosphere conditions. Based on these investigations, critical temperatures for lubricant removal are determined and optimum parameters for delubrication are proposed. Mathematical models have been developed which can predict the completion of the delubrication process [58], [76]. Owing to the complex nature of the delubrication process, in-situ monitoring methods to determine and control lubricant removal by adjusting the parameters accordingly are sought for. Monitoring systems for sintering furnaces equipped with sensors for oxygen, hydrogen, dew-point, carbon monoxide, carbon dioxide and methane exist [50], [77]. Using these sensors, closed-loop control systems have been implemented for sintering, which take readings from the furnace and regulate the composition and atmosphere flow rate to improve the sintering performance [78]. However, usage of sensors for atmosphere analysis in

the preheat zone is limited due to the volatile lubricants, high dew-points and sample line plugging [7]. Indirect observation of improper delubrication can be achieved through the CO/CH_4 sensors used in the hot zone detecting the presence of lubricant decomposition products that are not completely removed in the preheat zone and entering the high temperature zone.

Previous studies have indicated that monitoring gas-phase products is a reliable approach to monitor the delubrication process [7], [8], [12], [55], [58]. Using this approach, an in-situ delubrication monitoring means based on measuring the concentration of short chained hydrocarbon products during lubricant removal has been demonstrated [7], [55]. The concentration of the hydrocarbons is claimed to be indicative of the delubrication process as was seen from the combination of TG measurements and Raman scattering analysis during the progress of delubrication [10]. Since the lubricant is the only possible source for their origin, a drop in their concentration to a predetermined level is considered to be indicative of the completion of the process. This method is supported by a recent investigation where gas-phase products from delubrication were measured [67]. Practical application of this technique at an industrial scale for monitoring delubrication of EBS resulted in difficulties mainly due to the condensation of large molecular hydrocarbons blocking the sampling lines to the analyzer. The difficulties were lesser for monitoring the removal of polypropylene since it easily breaks down into smaller hydrocarbons [7], [55]. However, results from another study where pyrolysis products of EBS were studied suggest that monitoring small molecular hydrocarbons would not be representative for monitoring delubrication since their emission maxima occur at temperatures well below that of the emission maxima for the major decomposition products that were identified [8]. It has been suggested that delubrication-monitoring sensors would instead require detection of CO_2 or aliphatic hydrocarbons with an absorption range between 3000 and 2700 cm^{-1} based on the maximum concentration of various gases identified during the decomposition of EBS. It is further argued that CO and CO_2 formed during delubrication might be affected by catalytic effects due to the Fe/C base material in which case they might not serve as good indicators [67].

Effect of Delubrication on Sintering

Since delubrication precedes the actual sintering stage, changes induced during delubrication in terms of surface chemistry are carried over to the next stages and can have a direct impact on the final properties of the compacts after sintering. This effect being more pronounced when strong oxide forming elements such as chromium are present, has been one of the reasons for the choice of Astaloy CrM for performing the delubrication studies. Although there has been extensive research concerning the sintering of Cr prealloyed PM steels, detailed studies related to the changes in surface chemistry occurring during delubrication and their effect on the properties of the compacts after sintering have not been reported.

4 SINTERING

Thermodynamic considerations with emphasis on oxidation-reduction and carburization-decarburization reactions occurring during the sintering of chromium-alloyed PM steels are discussed in this chapter.

Sintering transforms green compacts into high-strength components. The strength is imparted and improved by the formation and development of inter-particle necks, which are metallurgical bonds formed between the particles. Mass transport for the neck formation during sintering can occur via surface or bulk transport. For the case of surface transport, atoms are transported from the pore surface while in bulk transport the migrating atoms originate from the interior of the particles. Surface transport hence does not result in dimensional change while bulk transport results in shrinkage [1]. For PM steels, surface diffusion is the most important transport process since it occurs at lower temperatures (compared to bulk diffusion) and results in strengthening of the compact without dimensional change.

For the inter-particle neck formation to occur, it is essential that the oxides covering the powder particles are removed, at least partially. For this purpose graphite is added to the compacts, which acts as a reducing agent apart from providing alloying. For successful sintering of PM steels it is essential to control both oxidation-reduction and carburization-decarburization reactions. With regard to chromium alloyed PM steels, N_2/H_2 mixes are recommended for sintering due to the oxygen sensitivity of chromium. Also, hydrocarbon additions are required for carbon control in such atmospheres, since precise carbon control is necessary for robust part manufacturing [54], [79]. Attention hence has to be given to the possible reactions, which occur involving several constituents such as carbon (graphite and dissolved carbon), oxygen, hydrogen, moisture, hydrocarbons, carbon monoxide and carbon dioxide when designing the sintering process. When several gaseous constituents are present in the sintering atmosphere, interactions in the furnace depend on the temperature and partial pressure of the constituents present. Varying temperature profile throughout the furnace results in varying carbon and oxygen potentials in the furnace. Low reactive atmospheres are preferred since the rate of undesirable reactions such as decarburization can be avoided [70]. However, the disadvantage with this approach is that the buffering capacity of the atmosphere is degraded.

4.1 Surface Chemical Characteristics of the Powder

As mentioned earlier, in order to achieve mechanical strength, bond formation is necessary between the particles for which oxides covering the powder surfaces act as diffusion barriers. Hence, an understanding of the surface state of the powder is essential to devise appropriate sintering. Previous investigations on the surface characteristics of water atomized chromium-prealloyed steel powder have shown that such powder is predominantly covered by a ~6-8 nm thick Fe- oxide layer along with the presence of fine particulate oxides rich in Cr, Mn and Si of the size of a few hundred nanometers [18], [80], [81]. The surface coverage by easily reducible iron oxide layer has been estimated to be around ~95% [20], implying that most of the particle contacts after compaction are at Fe-oxide interface rather than the stable oxide particulates,

19

hence implying good sinterability. The onset of formation of inter-particle necks is hence dependent upon the efficient reduction of the Fe-oxide layer. It was also estimated that the easily reducible Fe-oxide layer contains ~50% of the total oxygen content in the powder [20][82].

4.2 Reactions during the Heating Stage

Reduction of the surface oxides on the powders has to be accomplished during the heating stage of the sintering process. This depends on their thermodynamic stability, represented by the change in Gibbs free energy ΔG, which is controlled according to the concerned thermochemical reaction. In the absence of reducing agents, dissociation of oxides can occur represented by the reaction for dissociation of the oxides according to Eq.1:

$$\frac{2}{y} M_x O_y = \frac{2x}{y} M + O_2 \qquad \text{Eq.1}$$
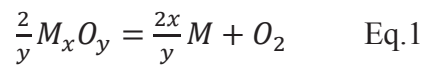
where M denotes the metal and $M_x O_y$ denotes the metal oxide. The change in Gibbs free energy for the reaction can be written as:

$$\Delta G_1^o = \frac{2x}{y} G^o(M) + G^o(O_2) - \frac{2}{y} G^o(M_x O_y) \qquad \text{Eq.2}$$

The equilibrium constant 'K' can be calculated according to Eq.3 based on Eq.1, where 'a' represents the activities of the constituents. The activity can be considered as unity for pure solids, which in this case are the metal and the oxide and hence only partial pressures of gas phases are included in the calculation of equilibrium constant and changes in Gibbs free energy.

$$K = \frac{a^{\frac{2x}{y}}(M) \times a(O_2)}{a^{\frac{2x}{y}}(M_x O_y)} \qquad \text{Eq.3}$$

$$\Delta G_1^{o} = -RT \ln K \qquad \text{Eq.4}$$

$$P(O_2) = \exp\left(-\frac{\Delta G_1^o}{RT}\right) \qquad \text{Eq.5}$$

The relation between the ΔG and equilibrium constant can be stated according to Eq.4. The temperature dependence of the equilibrium oxygen partial pressure can hence be represented by Eq.5, and graphically presented for the oxides of interest in Figure 6. Below each curve, oxide dissociation takes place while oxidation occurs at the values above it. The equilibrium oxygen partial pressures at the standard sintering temperature, 1120 °C, are marked in the figure for Fe_2O_3 and Cr_2O_3, respectively. The activities for metallic and oxide phases were considered unity for the calculations.
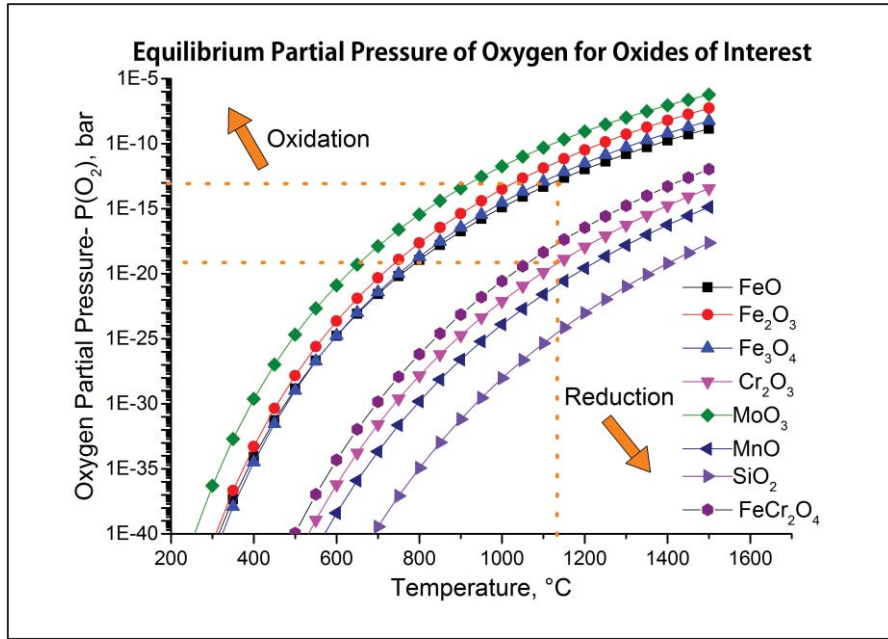
Figure 6 Equilibrium partial pressure of oxygen for the dissociation of oxides of interest

Considering the presence of graphite as the reducing agent, additional reduction reactions are expected to occur. Graphite can contribute to the reduction of the oxides either by direct or indirect carbothermal reduction according to Eq.6 and Eq.7, respectively.

$$\frac{2}{y}M_xO_y + 2C = \frac{2x}{y}M + 2CO \qquad \text{Eq.6}$$

$$\frac{2}{y}M_xO_y + 2CO = \frac{2x}{y}M + 2CO_2 \qquad \text{Eq.7}$$
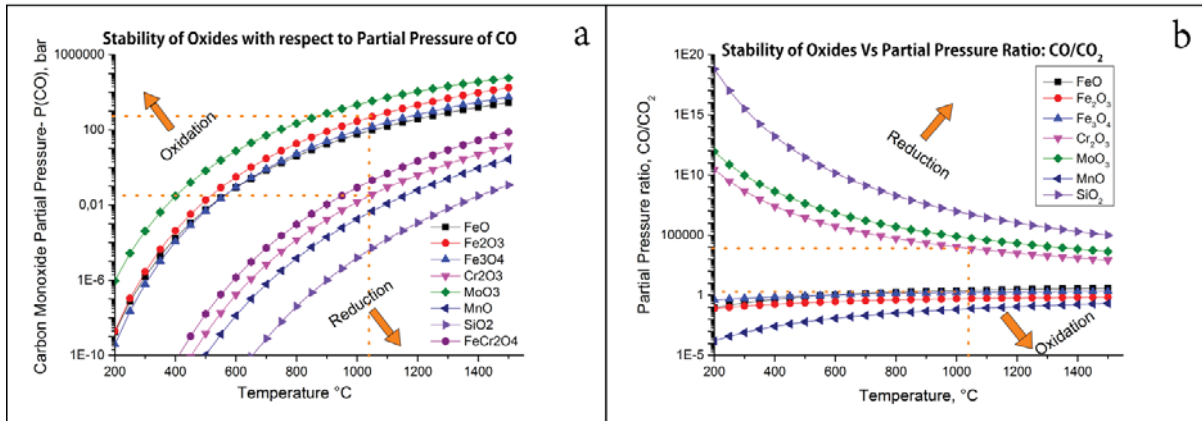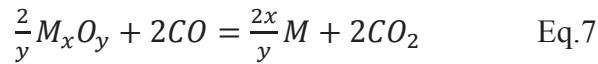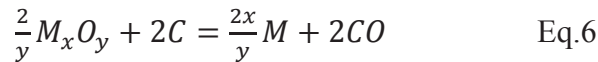
Figure 7 Equilibrium partial pressure of (a) CO and the (b) CO/CO₂ ratio with respect to the stability of oxides

Direct carbothermal reduction can occur where graphite and the oxide are in direct contact. Such contacts points being limited, the reaction is expected to play a secondary role. However, indirect carbothermal reduction can occur by means of the carbon monoxide that can be generated from graphite by its reaction with carbon dioxide produced by means of indirect carbothermal reduction reaction (Eq.8) or by its reaction with water vapor (Eq.9), the sources for which can be either the sintering atmosphere or the compact itself. The equilibrium partial

pressures for oxides with regard to direct and indirect carbothermal reduction reactions are plotted in Figure 7 and the stability values for Fe_2O_3 and Cr_2O_3 are marked. For the calculations, the activities for graphite, metallic and oxide phases were considered unity.

$$C + CO_2 = 2CO \qquad \text{Eq.8}$$

$$C + H_2O = H_2 + CO \qquad \text{Eq.9}$$
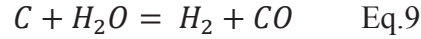
Once carbon monoxide is generated, it is expected to play the principle role in reduction and its generation is ensured by the 'Boudouard reaction' (Eq.8) which becomes thermodynamically favorable above ~720 °C. This reaction results in a volume increase of the gaseous constituents creating a protective atmosphere inside the compact providing favorable conditions for reduction, especially since carbon is more reducing than hydrogen at high temperatures [72]. Besides working reducing agents, graphite and carbon monoxide contribute to maintain the oxygen partial pressures at levels favorable for reduction inside the pores referred to as the "microclimate". It should, however, be emphasized that excess concentrations of carbon monoxide can result in oxidation as seen from Fig.7. The activity of carbon is unity during the heating stage since it is present as graphite. Apart from the reduction of the oxides, carbon dissolution into the metallic matrix of the compacts occurs during the heating stage, most probably according to the reverse reactions in Eq.8 or 9, with reaction according to Eq.9 being more intense [70], [83], [84]. Besides the reduction of oxide layers, for carbon dissolution to occur the temperature should be above the alpha-gamma transition temperature for the ferrous alloy. Although Boudouard reaction is favorable at ~720 °C, experimental studies show that the graphite becomes active only at temperatures around 900 °C and the dissolution and activity of graphite depend upon the carbon source [72], [83], [85]–[89]. Studies on reduction of hematite by graphite indicate that the rate-determining step was the gasification of graphite [90]–[92].

During the heating stage, at temperatures between 800 and 1100 °C, transformation of the easily reducible iron oxide into more thermodynamically stable Cr and Mn spinel oxides takes place [11], [19], [93]–[97] due to the increased mass transfer of the alloying elements at higher temperatures according to the model proposed in [19], [98]. This temperature range is hence considered critical [81], [98]. Further oxide transformations can be expected during heating to and holding at the sintering temperature. The transformation of the oxides according to their thermodynamic stabilities can be predicted to occur in the order mentioned below with the arrow marks pointing towards the more stable oxide [95], [99]. The spinel oxide $MnCr_2O_4$ can be considered as the most stable oxide phase present at typical industrial sintering conditions [95], [97].

$$Fe_2O_3 \rightarrow FeO \rightarrow Fe_2MnO_4 \rightarrow Cr_2FeO_4 \rightarrow Cr_2O_3 \rightarrow MnCr_2O_4 \rightarrow MnO \rightarrow MnSiO_x \rightarrow SiO_2$$

Presence of hydrogen is hence considered advantageous since it results in the reduction of the iron oxide present on the powder surfaces at lower temperatures, according to Eq.10, before oxide transformation occurs, thereby improving the neck formation [81], [98]. The oxide reduction due to hydrogen expressed by the relationship between the partial pressure ratio of hydrogen and water vapor with variation in temperature is shown in Figure 8a. The sintering

22

process with regard to the entrapment of oxides can also be addressed with the appropriate adjustment of the heating rate [100].

$$\frac{2}{y} M_x O_y + 2H_2 = \frac{2x}{y} M + 2H_2 O \qquad \text{Eq.10}$$
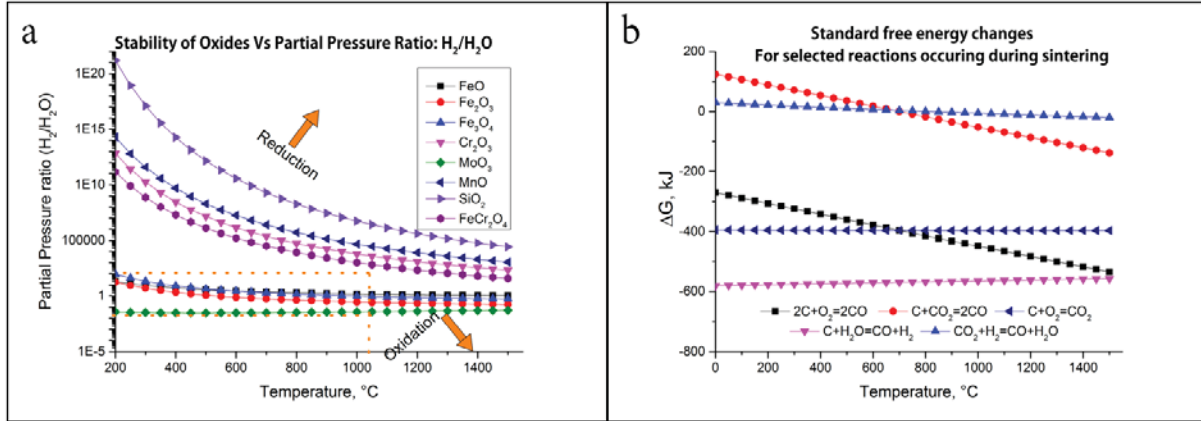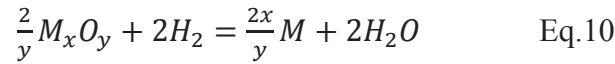
Figure 8 a) Equilibrium partial pressure ratio of H$_2$/H$_2$O for the stability of oxides, b) Standard free energy changes for selected reactions occurring during sintering

Another important reaction between CO, CO$_2$, H$_2$ and H$_2$O at favourable temperatures above ~850 °C is the water-gas reaction presented by Eq.11, according to which the H$_2$/H$_2$O and the CO/CO$_2$ ratios cannot be independently varied in the sintering atmosphere, see Figure 8b.

$$2H_2 + 2CO_2 = 2H_2 O + 2CO \qquad \text{Eq.11}$$
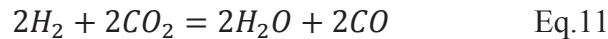
This also implies that there is no difference in measuring either of the ratios to ensure proper atmosphere control. It also suggests that increasing hydrogen content shifts the reaction towards more reducing conditions. Experimentally it was shown that the reduction of iron oxide by graphite for pure iron and iron-molybdenum powders occurs around 700 °C. For prealloyed powder, significant mass loss and reduction occurred only at temperatures above 900 °C, which indicates risk of the iron oxide transformation [72], [99]. For atmospheres containing hydrogen, iron oxide reduction is shown to occur at temperatures below 550 °C, according to Eq.10 [99], [101]. Nitrogen is generally regarded as an inert carrier gas but it should be mentioned that it can result in the formation of nitrides for chromium-alloyed PM steels [102].

4.3 Reactions at the Sintering Temperature

Further development of the inter-particle necks occurs during sintering. The transformation of the (entrapped) oxides can occur during sintering which according to their thermodynamic stabilities can be predicted to occur in the order mentioned above with the arrow marks pointing towards the more stable oxide [95], [99]. Oxide coalescence occurs during sintering as well [19], which is regarded as positive due to an increase in the cross-section of the metallurgical bond between two particles. With regard to the internal oxides, their reduction can occur only under high temperature sintering conditions i.e., at and about 1250 °C but are not affected at standard sintering conditions [72], [103], [104].

23

At the sintering temperature, the admixed graphite is completely dissolved in the matrix and the carbon content in the compact is determined by the carbon potential of the atmosphere. Ideally the sintering atmosphere is designed to be neutral at the sintering temperature while being slightly carburizing during cooling. Decarburization reactions occur due to the interaction of the dissolved carbon with the oxidizing constituents present in the atmosphere or in the compact according to Eqs.8 and 9. Nitrogen-hydrogen atmospheres with no water vapor offer neutral sintering conditions at the sintering temperature in theory, but oxygen from leakages in the furnace or the compact would react to form water vapor resulting in considerable decarburization, reaction according to Eq.9 being several orders of magnitude faster compared to that according to Eq.8 [105]. Carbon control is extremely critical without which a large spread in the final mechanical properties can be expected [54]. In such cases for carbon control, additions of hydrocarbon are considered, usually in the form of CH_4 [44], [78], [106], [107]. Carburization will then occur according to Eq.12.

$$CH_4 = C + 2H_2 \qquad\qquad \text{Eq.12}$$
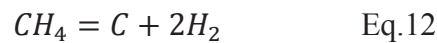
Carbon control can then be achieved, for example, by aiming at establishing a suitable rate between equations 8, 9 and 12. However, in practice, carbon control is executed through the measurement of free oxygen using a zirconia probe since it is more reliable compared to the measurement of dew-point, carbon monoxide or carbon dioxide contents using available sensors [70], [78]. Thermodynamic calculations show that hydrocarbon additions even in small amounts reduce the oxygen potential by several orders of magnitude when the molar concentration of hydrocarbons is higher than the water vapor concentration [108], [109]. At the same time, decarburization according to the reverse reaction in Eq.12 is expected for high hydrogen-containing atmospheres at high sintering temperatures [110]. The atmosphere carbon control is based on the assumption of equilibrium between gas phase and the compact. However, kinetics of reactions involving methane are also influenced by catalytic effects and therefore carbon control becomes difficult. For very low hydrogen concentrations and under extremely dry conditions, presence of excess methane would also result in soot formation. Propane can be used instead of methane to enhance the kinetics and to achieve the required carbon potential at four times lower concentrations [111]. Since lower concentrations would be sufficient to achieve the desired carbon potential with propane additions, the tendency of the atmosphere for sooting will decrease. It should also be emphasized, apart from reactions such as that mentioned in Eq. 12, other reactions can occur involving the hydrocarbons such as that mentioned in Eq. 13, the implications of which can be an improvement in the purity of the atmosphere.

$$C_3H_8 + 3H_2O = 3CO + 7H_2 \qquad\qquad \text{Eq. 13}$$
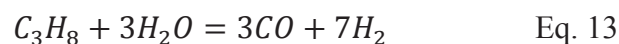
4.4 Cooling

After holding at sintering temperature, during cooling, the compacts are traditionally moved to a carbon restoration zone where carbon-loss is restored. The carbon potential of the atmosphere increases with decrease in temperature [78] and hence controlled carburization will occur if the temperature and carbon potential of the processing gas are well controlled [112]. Modern furnaces are equipped with sintering atmosphere control and this zone is utilized to achieve surface carburization in the compacts. Surface carburization can result in a compressive residual stress state which positively impacts the dynamic properties of the parts [113].

The main purpose of the following cooling zone is to establish the desired microstructure in the compacts by adjusting the corresponding cooling rates. The typical cooling rates achievable in modern belt furnaces are in the range of 1-3 °C/s. It is desirable that no further oxidation occurs in the compacts during cooling. This is achieved considering the counter-flow direction of the sintering atmosphere as the atmosphere purity is the highest in the cooling zone while it gets altered in the sintering and heating zones due to the products from the thermochemical reactions occurring in those zones. Furnaces equipped with cooling units which provide accelerated cooling can be utilized to perform sinter-hardening, where cooling rates up to 10 °C/s can be achieved [37], [114], [115].

For the case of CrM compacts admixed with 0.4 wt.% graphite, which is the materials studied in this thesis, considering a carbon-loss of 0.05 wt.% during sintering, the CCT curves for the material can be estimated using a materials property simulation software JMatPro (V.8) using the approach described in [116] , see Figure 9.
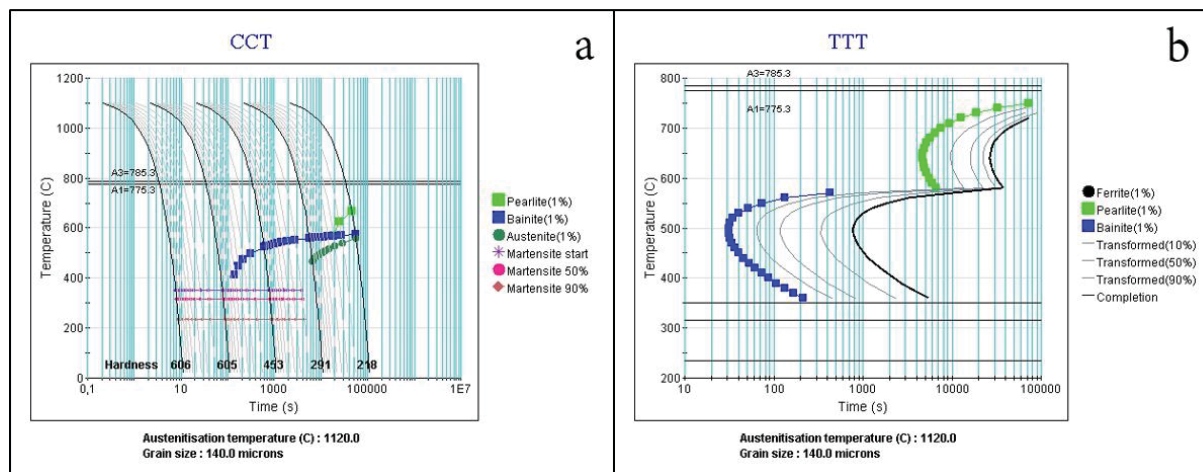
Figure 9 (a) CCT and (b) TTT diagrams for CrM+0.35C simulated using JMatPro 8.0

The corresponding phase compositions for the cooling rates used in this study- 0.16 and 0.5 °C/s and for the cooling rates corresponding to sinter-hardening 2.5 and 10 °C/s can be estimated as shown in Figure 10.

25
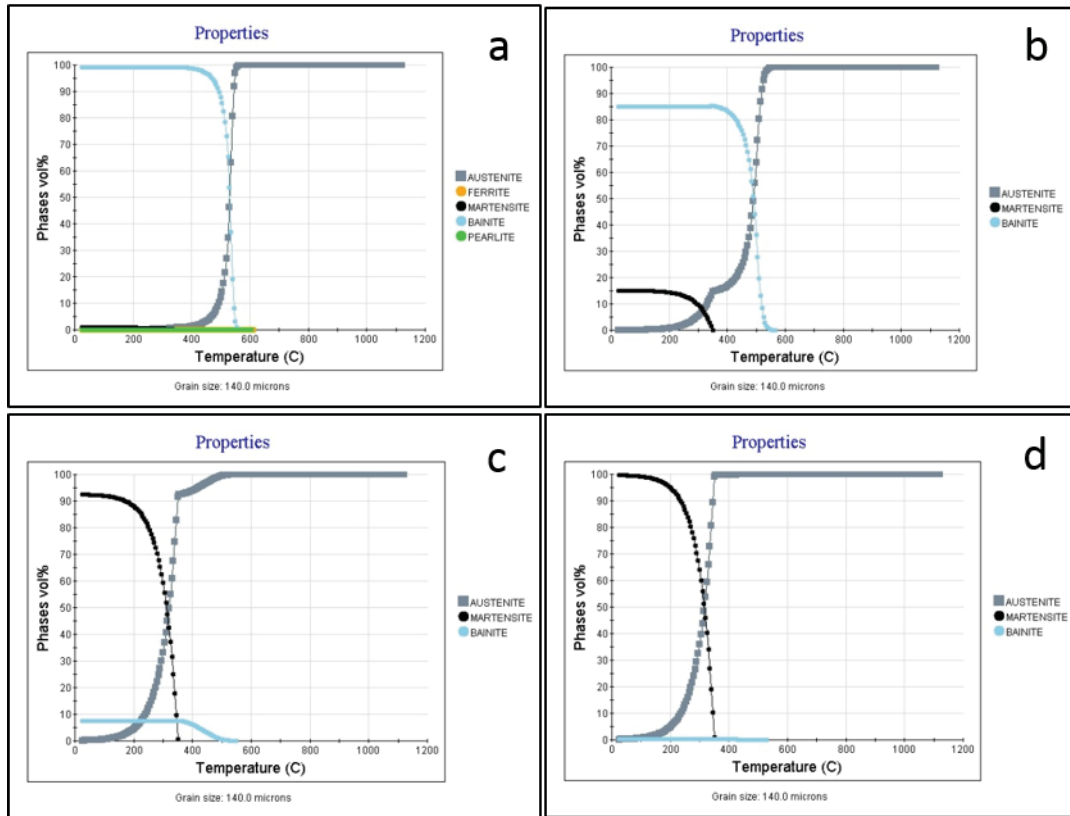
Figure 10 Phase compositions for CrM+0.35C corresponding to cooling rates a) 0.16 b) 0.5 c) 2.5 and d) 10 °C/s

In order to elucidate the effect of carbon content, which implies the importance of carbon control on the microstructure, the CCT diagram and phase compositions for a cooling rate of 0.5 °C/s for the case of 0.3 wt.% carbon are shown in Figure 11. It is important to note that even if relatively small changes in the phase composition are observed in later case, see Fig. 10 (b) and 11 (b), i.e., a decrease in martensite content by only 5 %, rather significant decrease is observed in terms of the hardness values, see Figs. 9 (a) and 11(a), connected to the lower carbon content in the resulting bainitic-martensitic microstructure.
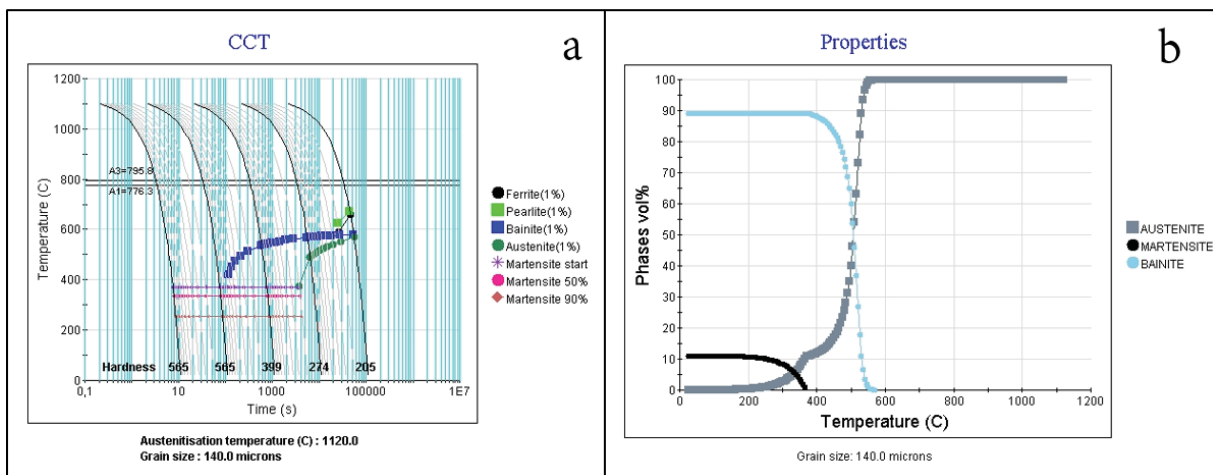
Figure 11 (a) CCT diagram and phase composition corresponding to a cooling rate of 0.5 °C/s for CrM with 0.3 wt.%C

4.5 Atmospheres containing Carbon Monoxide

It is suggested that sintering of chromium alloyed steels in endogas atmospheres is not appropriate due to the oxidizing effect of CO towards chromium, as can be seen from Figure 7 [72], [73], [99], [117]. However, apart from being economically attractive, endogas type atmospheres provide possibilities to intelligently introduce controlled carbon levels at the component surfaces which can result in favorable microstructures in terms of mechanical behavior. This is of an important consequence in terms of the carbon control as discussed in the previous sections. In such atmospheres, realizing high CO/CO_2 ratios can facilitate sintering of such powder, but there is a maximum obtainable ratio at any given temperature beyond which carbon deposition i.e., sooting, will occur [118]. $N_2/CO/H_2$ gases with varying contents of active reducing agents can be produced industrially by generated endogas atmospheres with diluted nitrogen or by dissociated methanol diluted with nitrogen [119]. The reverse reaction according to Eq.8 being kinetically prominent, utilizing low concentrations of the active constituents along with faster cooling rates in these atmospheres, indicate strong potential for carbon control [120]. For N_2/CO atmospheres, carbon monoxide would be the only carburizing and reducing constituent. For such atmospheres, the decarburization rate is lower. However, studies regarding sintering of PM steels in atmospheres containing carbon monoxide are scarce and hence are of interest.

5 RESEARCH OBJECTIVES

With the focus on sintering of chromium-alloyed PM steels, the objectives of this thesis study have been:

1) To develop a method for the assessment and control of the delubrication process by means of monitoring the process atmosphere utilizing sensors commonly used in the industry.
2) To perform a systematic study on the influence of various process parameters on delubrication using the method developed.
3) To investigate the effect of the delubrication process on the surface chemistry of the compacts and its impact on sintering.
4) To investigate the effect of the active components (CO, H_2, C_3H_8) in the sintering atmosphere on the reduction-oxidation and carburization-decarburization processes for chromium-alloyed PM steels.
5) To evaluate the possibilities for sintering chromium-alloyed steels in lean atmospheres containing carbon monoxide, hydrogen and hydrocarbon additions and to assess the effect of oxygen content in such atmospheres.

6 EXPERIMENTAL DETAILS

The main objective of this thesis have been to study the delubrication and sintering of chromium-alloyed PM steels for which Astaloy CrM has been chosen as the base powder. With regard to delubrication, the focus has been placed on method development based on processing atmosphere monitoring and surface analysis of the compacts after delubrication. With regard to sintering, the focus has been to study the effect of carbon monoxide and hydrogen containing atmospheres utilizing thermal analysis and sintering in laboratory scale.

6.1 Materials

Water-atomized steel powder prealloyed with 3 wt.% of Cr and 0.5 wt.% Mo has been the material primarily used in this study. It is a commercially available powder grade with the trade name *Astaloy CrM*, produced by Höganäs AB, Sweden. The delubrication and sintering experiments in this research were performed on Charpy impact test bars (ISO 5754: 10 ×10 ×55 mm) uniaxially compacted to a green density of ~7 g·cm^{-3}.

For the delubrication studies, the base powder was admixed with 0.6 wt.% of an ethylene bis-stearamide based lubricant (EBS_L). For the experimental work where the effect of graphite on delubrication and the effect of delubrication on sintering were studied, the compacts were admixed with 0.5 wt.% of natural graphite (UF4 grade, Kropfmühl). Additionally, compacts from a chromium-prealloyed powder grade with 1.8 wt.% of Cr, *Astaloy CrA*, with 0.5 wt.% of lubricant, compacted to ~7.3 g·cm^{-3}, were used to study the effect of density.

For the sintering studies two different sets of Astaloy CrM compacts, one without and one with 0.4 wt.% of admixed graphite were used. The base powder was admixed with 0.6 wt.% of ethylene bis-stearamide based lubricant (EBS_L) and delubrication was performed at 450 °C with a heating rate of 10 °C/min and a holding time of 30 minutes in dry N$_2$. The sintering experiments were performed on delubricated compacts utilizing different temperature profiles with the main focus on low temperature sintering at 1120 °C. In the experimental work where the main active component of the atmosphere was carbon monoxide, compacts based on pure iron powder, *ASC100.29*, were also used.

6.2 Process Atmosphere Monitoring

Delubrication experiments were performed in a laboratory tube (quartz) furnace *Entech* upon which a process atmosphere monitoring system was installed.

A schematic view of the experimental setup is shown in Figure 12. The process gas inlet tube was connected to a dew-point meter through a water bath which was placed on a heater for injecting moisture into the process atmosphere. This was used for performing experimental trials with wet atmospheres. The humidity of the inlet atmosphere was controlled by means of a ceramic dew-point sensor (Michel Cermet II). The process gas from the dew-point meter was flown through a flow meter where the flow of the gas into the furnace was regulated.

The monitoring principle is based on continuous on-line analysis of oxygen (zirconia ceramic sensor) and carbon dioxide (sensor based on infra-red cell technology) concentrations in the process atmosphere. The process gas flowing through the furnace was collected by means of a sampling tube placed in close proximity to the sample undergoing delubrication by continuous sampling using *Rapidox 3100A* dual O_2/CO_2 analyzer (Cambridge Sensotec Ltd). For the analyzer to function, the gas temperature entering the sensor should not exceed 55 °C. Hence, a stainless steel sampling tube was used, passing through which the temperature of the gas was reduced to acceptable limits before reaching the sensors. The sampled gas was then passed through a two-stage filtering system, which was installed to avoid sensor contamination. The first (coarse) filtration stage utilizes a stainless-steel pre-filter element for entrapment of particles >1 μm in size which includes the condensed heavy-hydrocarbons. The second stage consisted of microfiber filter element for the removal of particles of the size order of 0.1 μm. The dew-point meter was also used as a sensor for some process atmosphere monitoring experiments. Temperature measurement was simultaneously performed by a thermocouple (K-type) installed inside the specimen. The readings from the sensors and the thermocouple were then continuously logged during the process using a computer program.
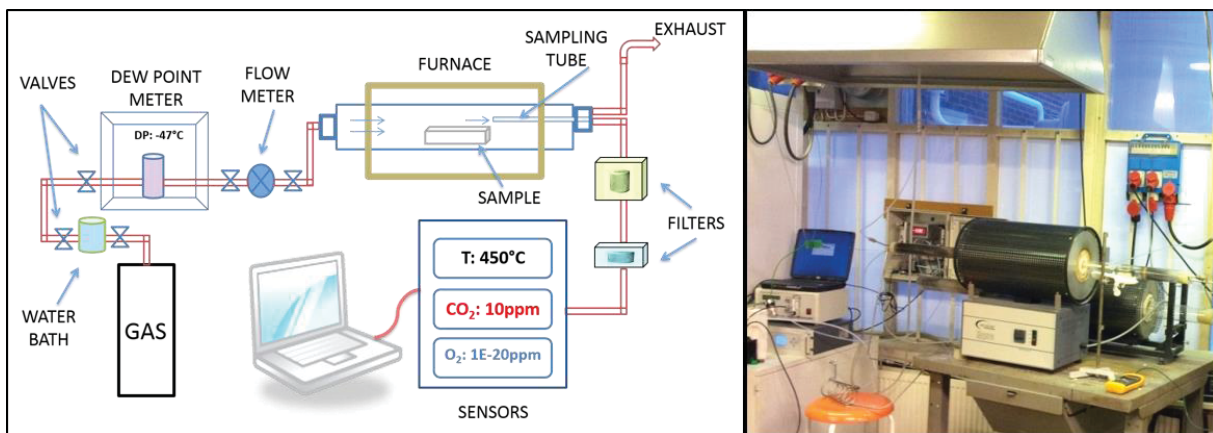
Figure 12 Schematic (Left) and Laboratory set-up (Right) of the Process atmosphere Monitoring System

Experimental Setup

Oxygen sensor

Solid ceramic electrolyte and acid/base electrolytic sensors are two popular oxygen monitoring devices used in the processing industry [77]. The oxygen sensor used in the experimental set-up for the present work is a solid ceramic electrolyte sensor. This sensor operates on a zirconia (ZrO_2) ceramic tube which is heated to temperatures around ~700 °C in the analyzer in order to facilitate oxygen ion conduction in the ceramic. The working principle is based on the difference in oxygen partial pressure between the sampled gas and a reference gas, generally air, generating an electromotive force between the electrodes which is measured. This is correlated to the oxygen content of the sample gas through the calibration of the sensor. The oxygen sensor used in this research provides analysis over the full range of oxygen partial pressures ($10e^{-20}$ ppm to 100% O_2). The advantage with ZrO_2 sensors is their quick response

32

time, easy maintenance and relatively low costs. For the sensor used in the present work, the response time was 5 seconds for a 90% response to a step change. Another important implication for using ZrO_2 sensors instead of oxygen sensors based on galvanic cells for monitoring delubrication is explained in detail in section 7.1.

Carbon dioxide (CO_2) sensor

Infrared (IR) sensors for CO_2 detection are spectroscopic devices used for gas detection which work based on the principle that each species absorbs IR radiation of a particular wavelength range. IR light is directed through a chamber containing the sampling gas to the detector. The CO_2 sensor provides high accuracy and stability in measurements with a response time of 30 seconds.

In-situ video monitoring

A video camera was installed for performing in-situ visual (video) delubrication experiments to track changes occurring through direct observation. The intention is to be able to correlate and validate the observations made using the process atmosphere monitoring (see Figure 13).

Figure 13 Setup and screen-shots from in-situ video of delubrication

Process parameters employed for delubrication studies

Employing the process atmosphere monitoring setup (see Figure 12) a systematic study of the effect of individual process parameters on delubrication has been performed. Influence of process atmosphere composition and purity, delubrication temperature, graphite addition, heating rate, flow rate, holding time and density were studied. Table 1 summarizes the processing conditions employed for the delubrication experiments.

Table 1 Processing conditions employed for the delubrication experiments

Variable	T, °C	Atmosphere	Heating Rate (°C/min)	Flow (Litres/min)	Dwell time (min)
Atmosphere	450	N_2 (dry), N_2 (wet), N_2+10H_2, N_2+0.3CO, N_2+H_2O, Air (dry)	~10	4	30
Temperature	900	N_2 (dry), N_2+10H_2, N_2+0.3CO	~10	4	30
	500 400 300	N_2 (dry)			
Graphite addition (0 and 0.5 wt.%)	450	N_2 (dry), N_2+10H_2, N_2+0.3CO	~10	4	30
	900	N_2 (dry), N_2+0.3CO			
Heating rate	450	N_2 (dry), N_2+10H_2, N_2+0.3CO	~10 ~20 ~30 ~50	4	30
	500 400 300	N_2 (dry), N_2+0.3CO			
Flow rate	500	N_2 (dry), N_2+0.3CO	~50	6,4,2,1,0.75, 0.5,0.25,No flow	30
	450	N_2 (dry)	~10	7.5 L/min	30
Holding time	450	N_2 (dry)	~10	4	0,10,20
Density (7.0-7.3 g/cc)	450	N_2 (dry), N_2+10H_2, N_2+0.3CO, Air (dry)	10	4	30
	900	N_2 (dry), Air (dry)			

34

6.3 Analytical Techniques

Thermogravimetry

Thermogravimetric analysis (TGA) involves determination of amount and rate of mass change for a material in relation to change in temperature in a controlled atmosphere. During the analysis, the temperature is increased according to the specified temperature profile so that one of the components undergoes a mass change for e.g., decomposition or evaporation. The weight of the sample is determined before the analysis and then the weight change with temperature/time is measured and a weight loss/gain curve is generated which is usually represented in terms of a relative mass change. Hence, the basic components of the analyzer consist of a sample holder, a high resolution balance system and a furnace chamber. The setup is vacuum-tight and ensures pure and well-defined atmosphere control during the measurement.
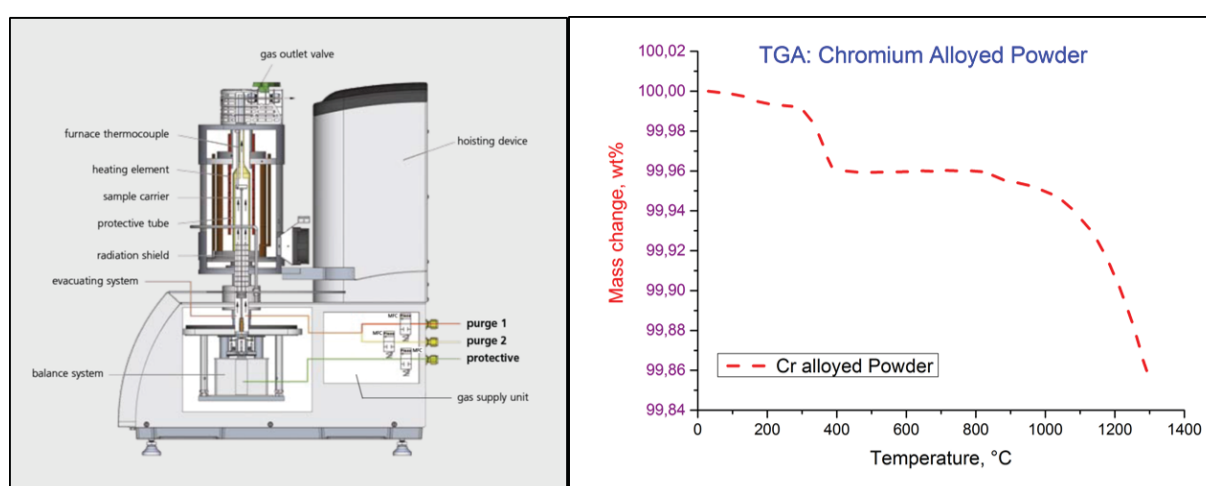
Figure 14 Left: Thermogravimetric Analysis Equipment set-up (with permission from NETZSCH Gmbh), Right: Example of the TGA curve (Authors own research)

The equipment used in the present work is a simultaneous *TG/DTA/DSC thermal analyzer STA 449 F1 Jupiter®* equipped with a high sensitivity balance system with high resolution in terms of weight and temperature measurement. A schematic view is shown in Figure 14. The equipment has a top loading design with an ultra-nano balance with a resolution of 25 ng. A W/Re thermocouple was used for monitoring the temperature. The TG sample carrier system was used since it allows for analysis of large samples, in our case ~5 g (including crucible). After loading the sample, before performing the experiment, the measuring system was evacuated three times and purged with argon (purity 6.0) before each test and an oxygen trap system OTS® was used to ensure the required gas purity and composition for some of the experiments.

For studies on lubricant removal, TGA was performed on both small pieces crushed from the compacts and pieces cut from the green compact by varying the process parameters. For the studies on the influence of sintering atmosphere composition on the CrM compacts, the samples

were dry cut into rectangular bars approximately $5 \times 5 \times 10$ mm or $10 \times 10 \times 3$ mm in size to obtain samples of ~2 g in mass. The samples used for the sintering studies were delubricated in dry nitrogen at 450 °C prior to the TGA studies.

Several gas compositions were used for the studies on the effect of atmosphere composition on the sintering of chromium-alloyed PM steel, which are tabulated in Table 2. The temperature profile employed for TGA analysis consisted of heating to a temperature of 1300 °C with a holding time of 30 min at a rate of 10 °C/min followed by a cooling at a rate of 30 °C/min. The gases used were supplied by AGA Gas AB and were of 99.9995 purity. An example of a typical thermogravimetry curve obtained for chromium-alloyed powder in hydrogen containing atmospheres is shown in Figure 14.

Table 2 Atmosphere compositions employed for TGA of the sintering process

Hydrogen	Carbon Monoxide	Carbon Monoxide and Hydrogen	Carbon Monoxide, Hydrogen, Propane	Carbon monoxide, Hydrogen, Propane, Oxygen
Ar-10 % H_2	Ar-10 % CO	Ar-10 % CO 20 % H_2	-	-
Ar-7.5 % H_2	Ar-7.5 % CO	Ar-7.5 % CO 15 % H_2	-	-
Ar-5 % H_2	Ar-5 % CO	Ar-5 % CO 10 % H_2	-	-
Ar-2.5 % H_2	Ar-2.5 % CO	Ar-2.5 % CO 5 % H_2	-	-
	Ar-1.5 % CO	Ar-1.5 % CO 3 % H_2	Ar-1.5 % CO 3 % H_2 10 ppm C_3H_8	Ar-1.5 % CO 3 % H_2 10 ppm C_3H_8 25 ppm O_2
Ar-1 % H_2	Ar-1 % CO	Ar-1 % CO 2 % H_2	-	-
	Ar-0.5 % CO	Ar-0.5 % CO 1 % H_2	Ar-0.5 % CO 1 % H_2 10 ppm C_3H_8	Ar-0.5 % CO 1 % H_2 10 ppm C_3H_8 25 ppm O_2
	Ar-0.1 % CO	Ar-0.1 % CO 0.2 % H_2	Ar-0.1 % CO 0.2 % H_2 10 ppm C_3H_8	Ar-0.1 % CO 0.2 % H_2 10 ppm C_3H_8 25 ppm O_2
Ar-50 % H_2	-	-	-	-
Ar-100 % H_2	-	-	-	-

Dilatometry

Dilatometry is a thermo-analytical technique usually used for the determination of dimensional changes (thermal expansion or shrinkage) occurring in materials as a function of temperature and/or time. It can be also used to perform rate-controlled sintering studies in powder metallurgy. In this study a horizontal pushrod dilatometer DIL402C equipped with a vacuum tight furnace supplied by Netzsch was used, see Figure 15. For performing the dilatometric analysis, the sample is inserted into the sample holder and a push rod is positioned directly against the sample, which transmits the length change recorded during the specified time-temperature cycle to a linear variable displacement transducer. The temperature program is controlled by a thermocouple located next to the sample. An example of the dilatometry curve obtained during cooling after sintering for a chromium alloyed PM steel compact is shown in Figure 15. The figure shows the presence of a phase transition indicated by a dimensional change and from the rate of which the corresponding phase transformation temperatures can be evaluated, which in this case is around 800 °C.
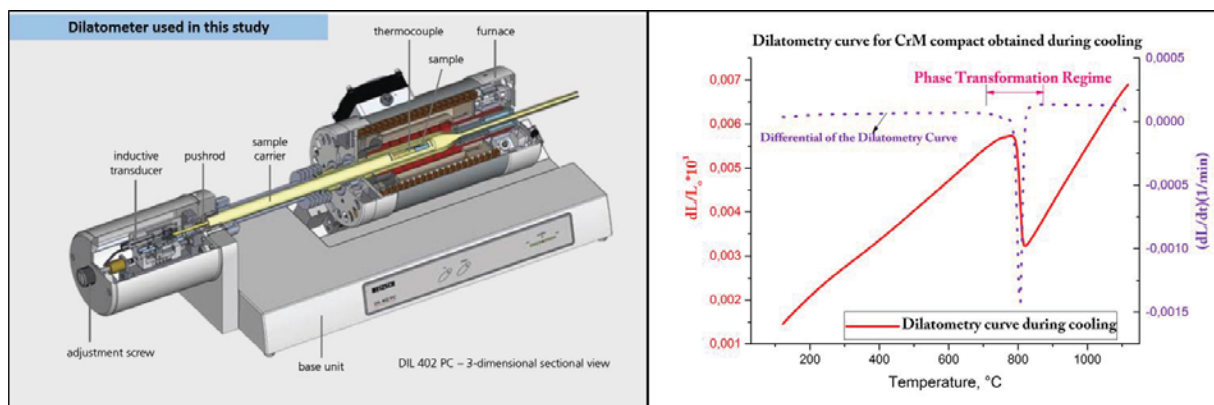
Figure 15 Left: Cross-sectional view of the dilatometer (with permission from NETZSCH Gmbh), Right: Example of a dilatometry curve obtained during cooling (from this work)

The dilatometer in this study was used mainly as a furnace with excellent control over the sintering atmosphere and temperature profiles. As in the case of the TGA, the setup was evacuated and flushed three times by Ar gas before the experiment. The sample holder in the dilatometer was devised to accommodate the Charpy impact test bar dimensions. The gas compositions employed for sintering in the dilatometer are tabulated in Table 3.

The thermal profile employed for sintering in dilatometer is heating to 1120 °C at 10 °C/min followed by holding at the sintering temperature for 30 min and cooling at a rate of 30 °C/min. Additionally, interrupted sintering trials were performed where the dwell time at the sintering temperature was 1 minute followed by cooling in Argon. In case of experiments with only Ar-CO gas mixes, interrupted sintering trials were also performed at 1000 °C for 1 min. For sintering in lean atmospheres consisting of CO, H_2, C_3H_8 and O_2, the sample geometry was modified to 30 mm×12 mm×2 mm. In case of lean atmospheres sintering trials at 1200 °C for 30 min were also performed.

Table 3 Atmosphere compositions employed for the sintering in the Dilatometer

Carbon Monoxide	Carbon Monoxide and Hydrogen	Carbon Monoxide, Hydrogen, Propane	Carbon monoxide, Hydrogen, Propane, Oxygen
Ar-10 % CO	Ar-10 % CO 20 % H_2	-	-
Ar-1.5 % CO	Ar-1.5 % CO 3 % H_2	Ar-1.5 % CO 3 % H_2 10 ppm C_3H_8	Ar-1.5 % CO 3 % H_2 10 ppm C_3H_8 25 ppm O_2
Ar-1 % CO	Ar-1 % CO 2 % H_2	-	-
Ar-0.5 % CO	Ar-0.5 % CO 1 % H_2	Ar-0.5 % CO 1 % H_2 10 ppm C_3H_8	Ar-0.5 % CO 1 % H_2 10 ppm C_3H_8 25 ppm O_2
Ar-0.1 % CO	Ar-0.1 % CO 0.2 % H_2	Ar-0.1 % CO 0.2 % H_2 10 ppm C_3H_8	Ar-0.1 % CO 0.2 % H_2 10 ppm C_3H_8 25 ppm O_2

X-ray Photoelectron Spectroscopy

X-ray photoelectron spectroscopy (XPS), also known as electron spectroscopy for chemical analysis (ESCA), is a surface sensitive technique, which is based on the principle that a surface irradiated by X-rays emits photoelectrons. In XPS, a low-energy X-ray beam is directed towards the sample which ejects electrons due to the photoelectric effect [121]. Soft X-rays with specific energies are used in order to excite the atoms of the material, placed in an ultra- high vacuum (UHV) environment, which emits characteristic photoelectrons. In an event where an electron from one of the core levels is ejected by the incident X-ray, the photon will have a kinetic energy (*KE*) given by the expression

$$KE = h\nu\text{-}BE\text{-}\varphi$$

where *hv* is the energy of the exciting radiation, BE is the binding energy of the emitted electron in the solid and *φ* is the spectrometer work-function. The kinetic energy of the emitted electron is measured by means of a hemispherical analyzer and thus the binding energy (*BE*) is calculated which is unique for each electron level for each element (see Figure 16).

One of the most important capabilities of XPS is its ability to measure shifts in binding energy of the core electrons resulting from changes in chemical environment, which can be due to the change in the nearest neighbor, oxidation state or compound characteristics. The emitted photoelectrons of interest have relatively low kinetic energies and hence have a higher probability of undergoing inelastic collisions with the atoms if they travel very far before leaving the surface. Thus only electrons originating from a few atomic layers below the surface will contribute to the XPS peaks making it a surface sensitive technique. This also describes the need for a high vacuum environment − UHV (<10^{-7} Pa). Typical analysis depth is

approximately between 3 to 10 nm, depending on the material. Since not only the energy but also the number of electrons for each energy interval is detected, proportionality between the surface elements present is created. Detection limit for the elements is typically in the parts per thousand ranges [122].
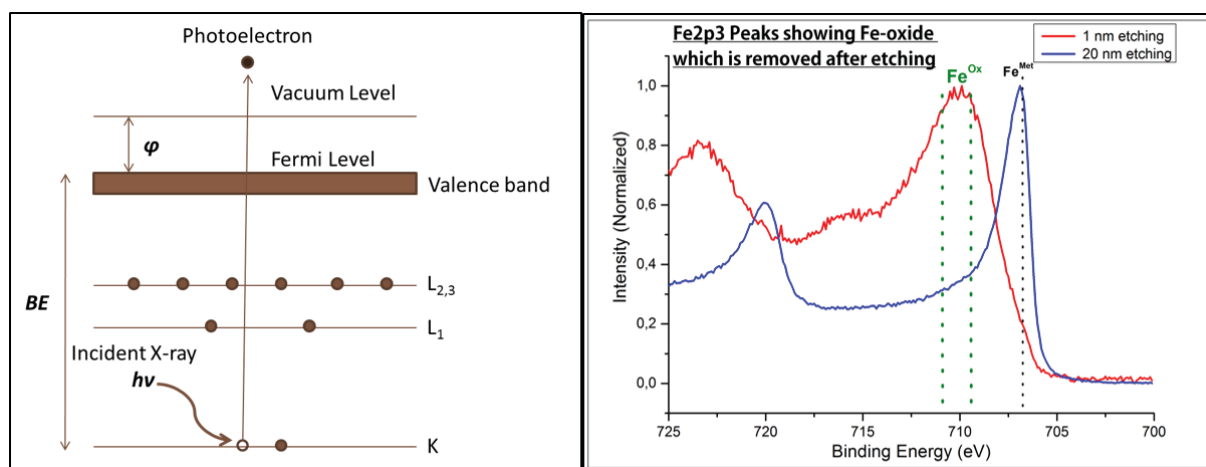
Figure 16 Left: Schematic of the principle of XPS, Right: An example of XPS spectra showing Fe-oxide and Fe-metallic peaks (authors' results)

In this study, XPS has been used for the determination of surface oxide layer composition and thickness as well as for identifying the chemical states of the elements present in the surface layer. The XPS analyses in this study were carried out by means of a PHI 5500 spectrometer operated using monochromatized Al Kα radiation source (hv=1486.6 eV). For the settings employed, the produced X-rays irradiate approximately an area of 0.8 mm^2 of the sample. The instrument is equipped with an ion-gun providing the possibility to perform depth profiling by means of which the oxide thickness and compositional profiles at different etch depths of the samples were obtained. In the present work, depth profiling is performed by Argon etching (Ar$^+$) over an area of 4×5 mm^2 with an etch rate of 2.85 nm·min^{-1}, calibrated on a Ta$_2$O$_5$ foil. An example of the XPS spectra corresponding to Fe showing its oxide chemical state after 1 nm etching (to remove surface contaminants) and after the removal of the oxide layer by etching is shown in Figure 16.

Scanning Electron Microscopy

In the present work, surface chemical analyses performed using XPS have been complemented with high resolution scanning electron microscopy (HR-SEM) combined with energy dispersive X-ray spectroscopy (EDS). SEM is widely used primarily because it provides high-resolution imaging combined with good depth of field imaging. In the SEM a beam of electrons is deflected to raster over a rectangular area on the sample. The electron beam is formed in an electron gun and the beam is focused by a lens system down to a nanometer width. Information is then collected by means of detectors located around the electron gun. A typical SEM setup can detect emitted electrons and scattered electrons, all which are products of the interaction of the electron beam with the sample in the interaction volume [123]. The energy of the electron beam typically ranges from 1 to 40 kV. By studying the photons emitted due to atomic excitation by the electron beam in the X-ray region, information about the elements can be

obtained since X-rays are characteristic and uniquely indicative of the elements of their origin. This is referred to as energy dispersive X-ray spectroscopy (EDX or EDS).

For the purpose of the present work, LEO 1150 Gemini equipped with a Field Emission Gun (FEG-SEM) and INCA Energy EDX analyzer is used. Since the analysis was to be performed on the surface of the powder or on the fractured surface of the compacts and the features of interest were sizing to the order of a few hundred nanometers, the parameters used for imaging and EDX analysis were: acceleration voltage of 15 kV and an aperture size of 20 μm with a working distance of 8.5 mm. The imaging was performed using an in-lens secondary electron detector as it provides high resolution and improved topological contrast at low beam voltages. An example of the appearance of the fracture surface in the SEM for Astaloy CrM is shown in Figure 17. The figure shows that the compact fractured in a dimple ductile fracture mode initiated by particulate oxides inside the necks along with the occasional presence of cleavage facets. In the high magnification micrograph, wavy step like features can also be observed on the free-powder surface, which are evaporation lines and their presence indicates a clean powder surface.
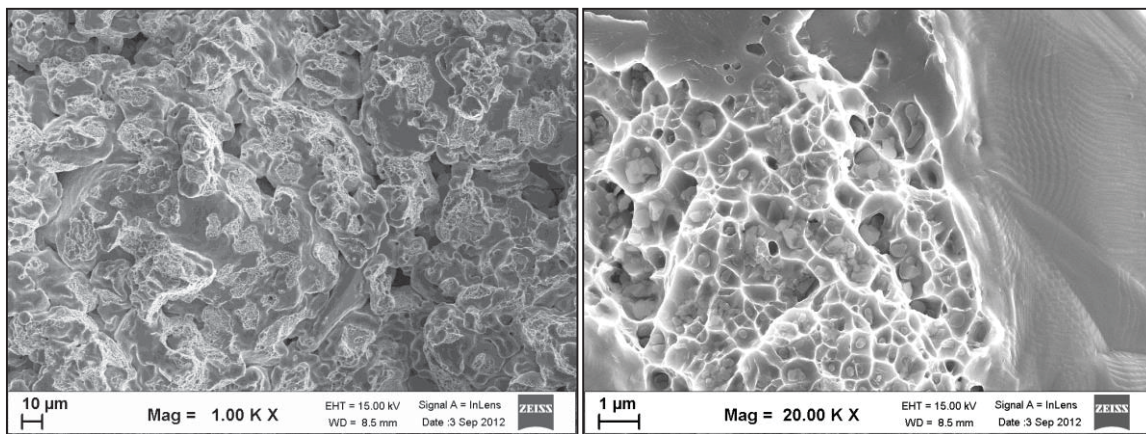
Figure 17 Left: Example of a fracture surface of a sintered CrM compact Right: High magnification image of the neck region and a clean free powder surface-showing evaporation lines

Chemical Analysis

The bulk chemical analysis for determining the carbon and oxygen contents was conducted using LECO TC-600 and LECO CS-844 instruments, respectively. For determining the oxygen content, the sample placed in a graphite crucible is melted in an induction furnace under flowing helium. The oxygen in the sample reacting with the crucible forms CO and CO_2, the presence and amount of which are detected by means of IR sensors. For the determination of carbon, the sample is combusted in an induction furnace under the flow of oxygen. From the CO and CO_2 evolved due to the carbon in the sample reacting with the oxygen, the amount of carbon is determined. These analyses were provided by Höganäs AB. Green compacts and chemical analyses for total carbon and oxygen concentrations for all the papers were provided by Höganäs AB.

7 SUMMARY OF RESULTS AND DISCUSSION

This thesis is based on the results from seven appended papers. Paper I focuses on the description of the method developed where sensors commonly used in the industry were employed for studying the delubrication process. In this study, the process atmosphere was monitored during delubrication and the gas concentration profiles from the sensors were correlated with the phenomena occurring during the individual stages in the lubricant removal process. In Paper II, a systematic investigation on the effect of individual parameters on the delubrication process was conducted and optimum parameters for the same were proposed. In Paper III, the influence of density on the delubrication process was studied using process atmosphere monitoring and correlating it with thermogravimetric analysis. Also, observations concerning the surface-chemical changes occurring in the compacts during delubrication by means of SEM-EDS investigations were discussed. The relationship between visual observation (in-situ video), thermogravimetric analysis and the process atmosphere monitoring of delubrication is described in Paper IV. The main focus of this paper was to examine the effect of delubrication process on the surface chemistry of the chromium-alloyed PM compacts and their impact on sintering. In Paper V, the influence of carbon monoxide in the sintering atmosphere on the reduction-oxidation and carburization processes with regard to chromium-alloyed steels was examined. In Paper VI, three different lean atmosphere compositions containing carbon monoxide, hydrogen, propane and oxygen as the active constituents were proposed for experimental studies based on thermodynamic calculations. The influence of the proposed atmospheres on the sintering of chromium-alloyed PM steels was investigated in this study. In Paper VII, the effect of hydrogen when present alone or as an addition to carbon monoxide containing atmospheres on the sintering of chromium-alloyed PM steels was assessed. The effect of propane additions to carbon monoxide and hydrogen containing atmospheres was also studied.

7.1 Process Atmospheres Monitoring: Method Development for Delubrication Studies

Since delubrication is performed as a part of the continuous sintering process, it is difficult to study lubricant removal and related aspects unless a set-up is established where delubrication can be investigated separately. For this purpose, an experimental system for monitoring the process atmosphere using industrial O_2, CO_2 and dew point (H_2O) sensors was built. The inlet process gas purity was controlled using the dew-point sensor in the set-up. The sample was heated to a specified temperature and the process gas was sampled continuously by means of a tube placed in close proximity to the sample and the signals from the CO_2 and O_2 sensors were recorded. A thermocouple was placed inside the sample (through a hole drilled) in order to record the temperature of the sample. In-situ measurements of the signals from the sensors were in this way logged through the process atmosphere monitoring set-up during the delubrication process. An example of such a profile is shown in the Figure 18.

From the process atmosphere monitoring profiles, it was noticed that the initial stages of delubrication are indicated by a drop in the oxygen partial pressure with an inflection point observed around ~270°C.
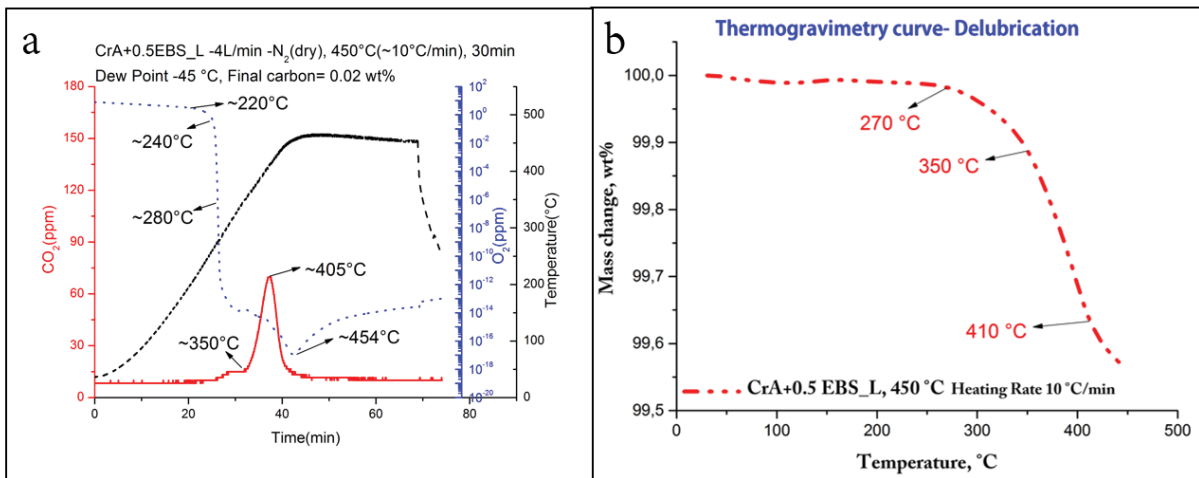
Figure 18 Left: Process atmosphere monitoring profile and Right: Thermogravimetry curve during delubrication (data from *Paper III*)

This significant drop in the oxygen partial pressure is connected to the working principle of the sensor which is based on ZrO_2 ceramic heated to ~700 °C to aid oxygen ion transport as described in section 6.2. Delubrication products reaching the sensor burn on the hot sensor surface consuming oxygen and contribute to a decrease in the recorded oxygen concentration (see Figure 19). Hence, the drop in the partial pressure hence is indicative of the presence of delubrication products from which the beginning of the lubricant removal can be inferred.
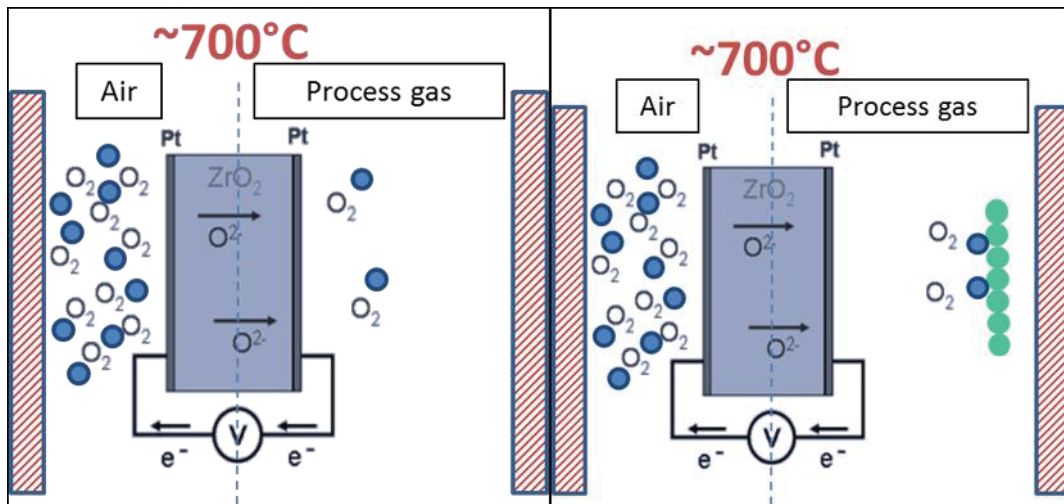
Figure 19 Schematic illustration of the indication of beginning of lubricant removal by the oxygen sensor

The oxygen sensor, however, proved ineffective when used in reducing atmospheres. This is because of the reaction of the active reducing agents in the atmosphere (in this case H_2/CO) with the oxygen present on the surface of the sensor lowering the partial pressure and not necessarily representing the actual constitution of the atmosphere.

Visual means were also employed to study the delubrication process and a video of the changes occurring during lubricant removal was obtained. Screenshots from the visual inspection of the delubrication process are shown in Figure 20. During visual observation of the delubrication process, no changes were observed until the sample temperature reached ~180 °C. When the sample temperature was around ~180 °C, appearance of transparent droplets was observed on the compact surfaces (*Paper IV*). With an increase in temperature, the droplets grew in number and slowly changed from being transparent to brownish. These changes were observed between 200-220 °C. Around 250 °C, size of the droplets increased and their coalescence was observed. Evaporation of the droplets was observed around 280 °C starting at the right end of the sample which is at a slightly higher temperature compared to the rest of the sample. Some deposits and white smoke were observed in the tube (of the furnace) starting around the same temperature. This temperature corresponds very well with the inflection point observed in the signal from the oxygen sensor as shown in Figure 18, reinforcing the idea that the initial stages of lubricant removal can be monitored using the oxygen sensor. Evaporation of the droplets continues until the temperature reaches 350 °C after which all the droplets were seen to disappear. Above 350 °C no visual changes were observed.

Figure 20 Screen-shots from the video taken during different stages of delubrication of the sample

No changes were observed in the CO_2 signal during the initial stages of delubrication. This is hypothesized to be due to the initial stages of lubricant removal at lower temperatures involving lubricant evaporation and decomposition forming heavy hydrocarbons that are not converted to CO_2 due to the lack of oxygen in dry atmospheres. The oxygen level further decreases with an increase in temperature and has a maximum slope at ~300 °C representing intense decomposition/evaporation of lubricant and reaches a minimum value around the temperature where it coincides with the peak on the CO_2 signal. CO_2 signal with a peak occurring around ~410 °C indicates second stage of delubrication involving decomposition into lighter hydrocarbons and carbon dioxide, etc. An increase in the oxygen concentration was observed during dwelling at the delubrication temperature but it does not reach the oxygen level characteristic of the nitrogen gas purity used. This increase in oxygen content was attributed to be due to the slow removal of the hydrocarbons which condense on the walls of the sampling system. Additional weak CO_2 peaks occurred around ~600 °C and 800 °C when the process temperature was increased to 900 °C which are associated with the carbothermal reduction of the surface oxides by the residues of carbon from the lubricant. For the samples admixed with graphite, these peaks were more intense. However, increasing the temperature to 900 °C did not change the character of the first CO_2 peak.

Thermogravimetry Studies

Thermogravimetric analysis was performed where the compacts were heated to 450 °C with heating rate of 10 °C/min. It was noticed that the critical points (temperatures) on the mass loss curve from thermogravimetry correspond well with the critical points obtained from the process atmosphere monitoring. Almost all the mass loss occurred during the heating stage. This suggests that the holding time can be significantly shortened. The observations from process atmosphere monitoring were in good correlation with the results obtained from in-situ visual observation (video of the whole process), thermogravimetric analysis and the bulk carbon and oxygen analyses of the compacts, see Figure 18.

7.2 Effect of Process Parameters on Delubrication

Using the process atmosphere monitoring set-up, the effect of individual parameters on the delubrication process has been evaluated.

Process atmosphere

It was shown that the effect of process atmosphere composition on the delubrication process in the case of inert and reducing atmospheres was minimal. The CO_2 peak was shown at around ~410 °C independent of the composition and purity of the atmosphere, except for the case where delubrication was performed in air. In the latter case, the peak shifted to higher temperatures with a multifold increase in intensity. This shift was attributed to the burning of the condensed delubrication products in the sampling system. The influence of moisture was observed to be minimal. A shoulder on the CO_2 peak was observed for the case of processing in air and for the case of wet atmosphere, which coincides with the intense evaporation peak on the oxygen signal.

Temperature

Increasing the temperature to 900 °C for delubrication did neither alter the position of the CO_2 peak nor the inflection points on O_2 signal. This was confirmed by results from the chemical analysis on the samples which showed that the content of carbon and oxygen obtained was similar to that for the case of delubrication at 450 °C.

Graphite Addition

Addition of graphite did not have an influence on the peak positions on the process atmosphere monitoring profiles suggesting that its influence is minimal. For the samples heated to 900 °C, addition of graphite resulted in more intense, additional peaks owing to the effective carbothermal reduction reactions.

Heating Rate

The samples were subjected to high heating rates (up to ~50 °C/min) by introducing them into the furnace preheated to a set (delubrication) temperature to simulate the situation of processing

in a batch furnace. A clear shift in CO_2 peak towards higher temperatures with an increased heating rate was observed, suggesting that the delubrication process has to be performed at higher temperatures (~500 °C) in such cases. From the O_2 signal, it was seen that the melting/evaporation process is accelerated, which increases the risk of formation of green-cracks.

Flow rate

When the flow was increased from a nominal 4 L/min (~0.04 m/s) to higher values (~0.08 m/s) it was seen that the intensity of the CO_2 peak decreased but the position remained the same, suggesting that the increase in flow does not influence delubrication. When the flow was decreased below the nominal value to nearly static flow conditions, the sample surface still remained clean after delubrication at 500 °C. However, when the temperature was decreased further to 400 °C, deposition of delubrication products was observed on the sample surfaces and the situation worsened on decreasing the temperature further to 300 °C. Atmosphere monitoring results showed that the process is incomplete at 400 °C and more so for 300 °C. Furthermore, at 300 °C, carbon dioxide peak was absent, suggesting that the decomposition reaction does not start at this temperature. Also, higher residual carbon content (lubricants and decomposition products) was observed in these compacts after delubrication confirming the same.

Holding Time

Results from chemical analysis and thermogravimetry indicate that almost all the lubricant is removed during the heating stage. Holding time at 450 °C did not significantly influence the residual carbon content in the specimen and this was in the range of around 0.02 and 0.04 wt.% independent of the holding time (0, 10, 20 and 30 min). However, holding time is recommended to account for the case when massive parts with complex geometry are used. Additionally, industrial furnaces have considerably higher load, meaning that additional holding time is required to assure proper purging-off of the lubricant/decomposition products.

Density

Independent of the atmosphere composition and temperature, it was observed that an increase in the density of the compacts from 7.0 to 7.3 g/cc did not affect the delubrication process. The only difference observed was in the intensity of the CO_2 signal, which was lower than that for the case of lower density samples. This is related to lower amount of lubricant added in the case of high-density samples, i.e., 0.5 wt.% instead of 0.6 wt.% used for samples with a density of 7 g/cc.

7.3   Changes in Surface Chemistry during Delubrication

Three different delubrication conditions were chosen where the changes in surface chemistry of the compacts were studied. The parameters considered optimum for delubrication based on process atmosphere monitoring were employed for the first condition, i.e., delubrication at 450

45

°C with a heating rate of 10 °C/min in dry N_2 and a holding time of 30 minutes at the delubrication temperature. In the second case, air was used instead of nitrogen in order to study the effect of oxidizing constituents in the process atmosphere on the surface chemistry and also to simulate the burn-off process. In the third case, delubrication temperature was increased to 900 °C keeping other parameters similar to those in the first case. Temperatures in this range employed industrially for delubrication motivated this choice of parameters.

Delubrication in N_2 at 450 °C resulted in a surface condition similar to that of the base powder. For the case of delubrication at 900 °C, though the bulk oxygen content in the compact remained similar to the previous case, the surface chemistry was altered. The concentration of Cr and Mn on the powder surface, present in their oxide states, significantly increased, which is related to the growth of undesirable thermodynamically stable oxides at the expense of pre-existing Fe-oxide layer. Delubrication in air at 450 °C resulted in a radical increase in the thickness of the oxide layer around the edges of the sample. From high resolution SEM imaging on the sample, oxide thickness exceeding 100 nm (in comparison with initial thickness of 6 nm) could be shown.

Influence of Delubrication on Sintering

The delubricated samples (from section 7.3) were subjected to sintering at 1120 °C in 90Ar-10H$_2$ atmosphere in a dilatometer to obtain controlled sintering conditions. Along with these samples, another sample which was delubricated at 300 °C in N_2 under static flow conditions at a higher heating rate was also sintered. The compacts sintered after delubrication at 300 °C resulted in inferior mechanical properties (impact energy: 9 J and hardness: 255 HV) and showed high bulk oxygen content. Presence of heavily oxidized regions resulting from poor microclimate due to the residual lubricant was proposed to be responsible for the inferior properties. The samples sintered after delubrication at 450 °C showed high impact energy (16 J) and hardness values (267 HV) along with a low carbon loss and final oxygen content. This is attributed to the surface state of the powder remaining unaltered after delubrication. After sintering, the compacts delubricated at 450 °C in air had the lowest impact energy (7.5 J) and hardness values (255 and 225 HV at center and edge respectively). This was suggested to be due to the higher carbon "spent" (carbon loss) for the reduction of the thick iron oxide layer formed during delubrication. The compacts delubricated at 900 °C in the as-sintered state showed lower impact energy (12.5 J) and hardness values (262 HV). Additionally, higher oxygen content and carbon loss were observed in these compacts. The higher oxygen content was related to the presence of the thermodynamically stable oxides and the lower impact energy was related to the presence of heavily oxidized necks resulting from the entrapment of Cr-Mn spinel oxides formed during the delubrication stage.

7.4 Role of Active Components in the Atmosphere during Sintering

Carbon Monoxide

The compact-sintering atmosphere interactions when carbon monoxide is the only active constituent in the atmosphere were studied in *Paper V*.

46

Atmospheres containing carbon monoxide exhibited both oxidizing and carburizing conditions with respect to chromium-alloyed PM steels during the heating stage of the sintering process until temperatures around 1000 °C. This was observed in the form of mass gain that increased with an increase in the concentration of carbon monoxide in the atmosphere from TGA. Examples for a mass change curve from the TGA and a micrograph corresponding to a compact without admixed graphite sintered at 1120 °C in an atmosphere containing carbon monoxide alone as the active constituent are shown in Figure 21. Carburization was evidenced by metallographic examination depicting bainitic or presence of pearlitic/bainitic microstructures when heating compacts without admixed graphite to 1000 °C. Graphite dissolution in the matrix was incomplete at these temperatures since fully bainitic microstructure was not observed for the compacts with admixed graphite. Further, oxidation in the form of Cr rich particulate oxides and Fe-oxide were observed on the fractured surfaces of the compacts.
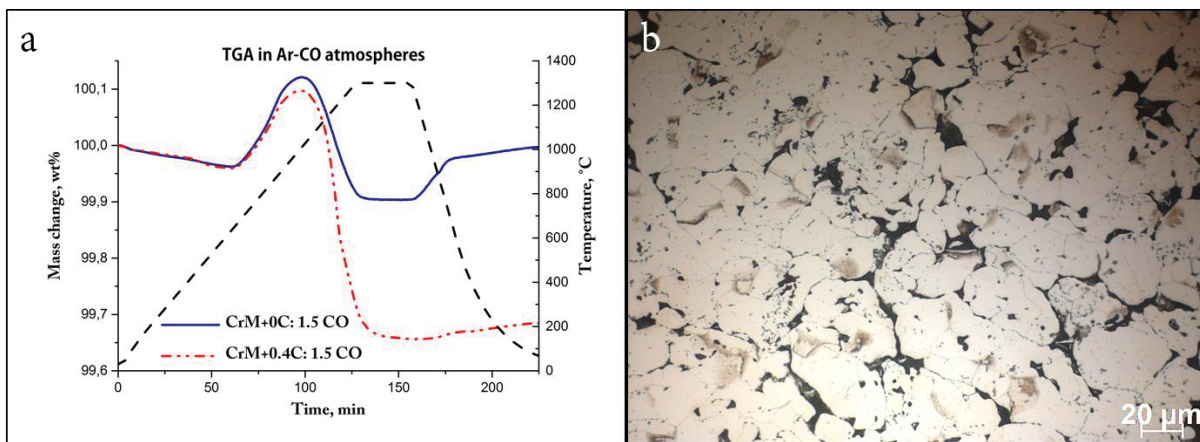
Figure 21 Left: TGA curve for CrM compacts for Ar-1.5 CO atmosphere Right: Microstructure of a compact without admixed graphite after sintering at 1120 °C for 1 minute *(based on data from Paper VII)*

Upon further heating to 1120 °C, the carbon and oxygen concentrations decreased in the compacts suggesting the effectiveness of carbothermal reduction at these temperatures. A mass loss was correspondingly observed in the temperature range of 1050 and 1300 °C, which was higher than the mass gain in magnitude when the carbon monoxide concentration was below 5 vol.%. For the compacts with admixed graphite heated in 0.1 vol.% CO to 1120 °C, fully bainitic microstructures were observed while bainite was observed only at the edges extending up to 1 mm from the edges when the atmosphere contained 1 vol.% CO. For the compacts corresponding to an atmosphere with 10 vol.% CO, the microstructure was ferritic-pearlitic. This is hypothesized to be due an increase in the temperature at which the atmosphere becomes reducing with respect to chromium with an increase in the carbon monoxide content as was seen from thermodynamic calculations.

Sintering at 1120 °C for 30 min resulted in homogeneous bainitic-martensitic microstructures for all the compacts containing carbon (graphite) after cooling. Fractographic analysis and bulk chemical analysis showed that the compacts sintered in 0.1 and 1 vol.% CO exhibit satisfactory properties after sintering. During holding at 1300 °C, no significant mass changes occur. During cooling, a mass-gain was observed for the compacts which was higher (twice in some cases) for the compacts without admixed graphite. This suggests that carburization should be a part of

the mass gain during cooling. However, the mass gain continues even towards lower temperatures suggesting that oxidation also occurs during cooling.

The effect of hydrogen when present as the sole active constituent and when present in combination with carbon monoxide were studied in *Paper VII*. Also, the effect of propane additions to atmospheres containing carbon monoxide and hydrogen was studied.

Hydrogen

When hydrogen is the only active constituent in the sintering atmosphere, multi-stage reduction was observed.
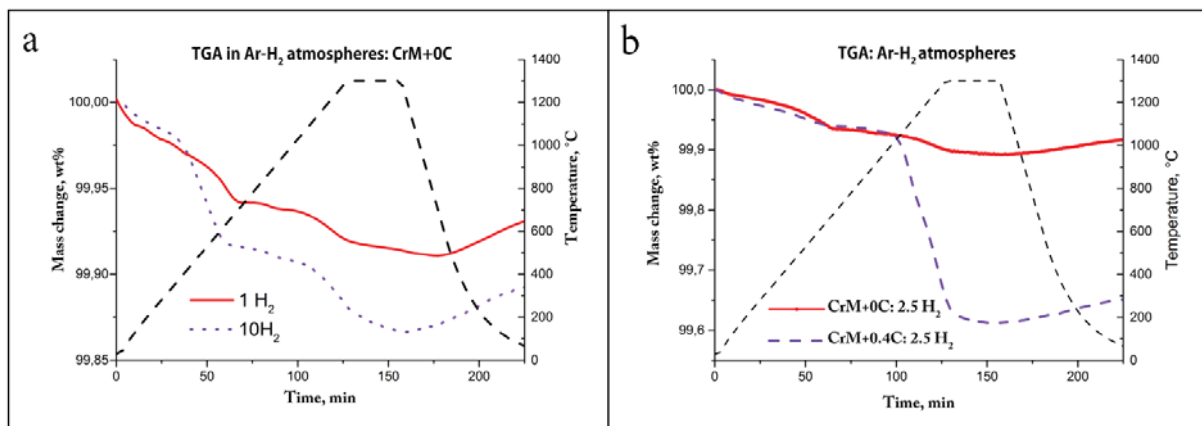
Figure 22 TGA for compacts in hydrogen containing atmospheres Left: compacts without graphite Right: effect of graphite addition *(based on data from Paper VII)*

Hydrogen contributes to the reduction of Fe-oxide at temperatures below 650 °C, the effectiveness of which increased with an increase in the concentration of hydrogen in the atmosphere. At temperatures above 800 and 1200 °C reduction of Fe-rich/spinel oxides and internal oxides takes place, respectively. When graphite was additionally present in the compacts, it becomes the dominant reducing agent even in hydrogen-rich atmospheres. This phenomenon is depicted in Figure 22.

Carbon Monoxide and Hydrogen

The TGA curves for the atmospheres containing carbon monoxide and hydrogen exhibited behaviour similar to that when carbon monoxide alone was present, signifying the prevailing effect of carbon monoxide in the atmosphere. From TGA of the compacts with admixed graphite, when compared to atmospheres with carbon monoxide as the only active constituent, in atmospheres containing additional hydrogen, the mass gain (both during heating and cooling) was higher and the mass loss was lower as can be seen from Figure 23. This was related to higher carburization and lower oxidation in the case of the latter. This suggests that the buffering capacity of atmospheres containing carbon monoxide can be improved by hydrogen additions. Additionally, the peak temperatures from the TGA curves were lower in the case of the latter suggesting that the reduction begins at lower temperatures. For the compacts without admixed graphite, the mass gain exhibited a non-linear trend when hydrogen was additionally

48

present which is hypothesized to be due to the competing effects of oxidation and reduction from carbon monoxide and hydrogen respectively.
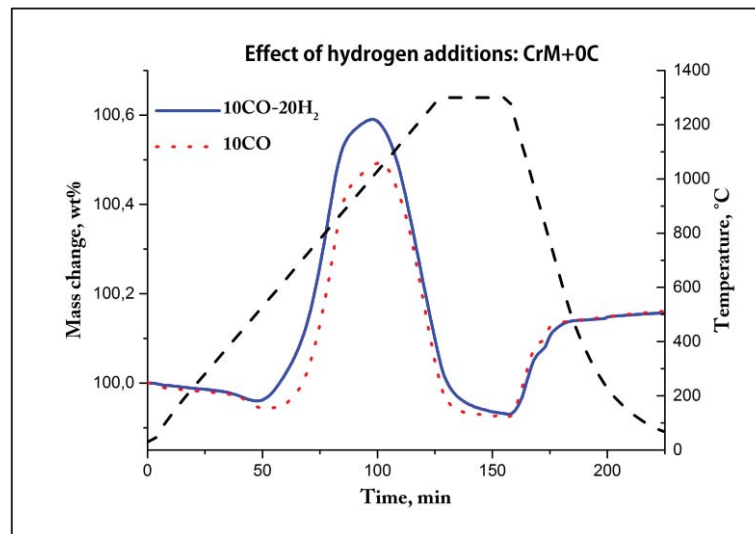
Figure 23 TGA of CrM compacts showing the effect of hydrogen additions to atmospheres containing carbon monoxide *(based on data from Paper V and Paper VII)*

Also, the samples sintered in carbon monoxide and hydrogen containing atmospheres at 1120 °C exhibited improved carburization and reduction compared to those sintered in atmospheres where carbon monoxide was the only active constituent.

Carbon Monoxide, Hydrogen and Propane

Propane additions to the carbon monoxide and hydrogen containing atmospheres did not have a significant effect. The temperatures corresponding to the maximum mass gain were shifted towards higher values but the mass gain and mass loss were observed to be lower. The oxygen content in the compacts after sintering was lower when propane was additionally present while the carbon content was not significantly different.

7.5 Lean Atmospheres for Sintering of Chromium Alloyed PM Steels

Studies concerning sintering of chromium alloyed PM steels in lean atmospheres are reported in *Paper VI*.

For atmospheres containing CO, H_2 and small amounts of hydrocarbons as the active constituents with their total concentration not exceeding 5 vol.%, thermodynamic calculations were performed to estimate the reducing and carburizing activities. These calculations showed that lean atmospheres containing only carbon monoxide exhibited poor buffering capacity, which can be improved by the addition of hydrogen (even in small quantities). Addition of hydrocarbons was shown to improve the reducing activity of the atmospheres containing hydrogen and carbon monoxide to an extent favourable for the reduction Cr-oxide at sintering temperatures. Based on these results, three different atmosphere compositions were proposed which can be represented in the form: N_2-*x* vol.% CO- *2x* vol.%H_2- 10ppm C_3H_8- 25 ppm O_2 with x=0.1, 0.5, 1.5 and are referred to as C-1, C-2 and C-3, respectively.

The carburizing ability of the proposed atmospheres was substantiated from the presence of pearlitic, and in some cases bainitic microstructures in the compacts without admixed graphite sintered in these atmospheres. This was complemented by the results concerning the phase transformation temperatures inferred from the dilatometry curves. Carburization was achieved in order as C-3> C-2> C-1 for all the sintering conditions studied. This was attributed to the concentrations of CO and H_2 in the atmospheres, which follow the same order. For the compacts with admixed graphite, pearlitic and/or bainitic microstructures were observed even after just 1 minute of holding at 1120 °C. This suggests that the atmospheres provide conditions suitable for the reduction of the iron oxide on the powder surfaces which is a prerequisite for the diffusion of carbon into the material matrix during the heating stage. The carbon content was lower for the compacts sintered in C-1 and C-2 atmospheres, compared to N_2-H_2 blend, which is hypothesized to be due to the lower carbon loss in the case of the latter. For the case of C-3 atmosphere, the carbon content obtained was higher compared to that for the N_2-H_2 blend, which could be due to its stronger carburization. The oxygen concentrations for the compacts with admixed graphite were much lower compared to those of their counterparts with no graphite, suggesting that graphite is the main source for reduction at high temperatures even when hydrogen is present.

For the compacts with and without admixed graphite, carbothermal reduction was effective during holding at the sintering temperature. During cooling, carburization of the compacts was observed and was shown to increase with decrease in cooling rate. Additionally, oxidation tentatively occurred during cooling and this was attributed to the oxidizing effect of carbon monoxide and residual oxygen present in the atmosphere. It was suggested that propane, which can react with the inherent oxygen in the atmosphere might be inactive at lower temperatures. Sintering of the compacts was performed after preheating the atmospheres by flowing them through a tube held at 1120 °C, which resulted in improved carburization and reduction. This validated the hypothesis concerning propane being inactive at lower temperatures and also served as a potential method to improve the performance of the proposed atmospheres.

8 CONCLUSIONS

8.1 Delubrication Method Development

- A method for studying delubrication has been developed based on monitoring the process atmosphere using industrial CO_2 and O_2 sensors.
- The initial stages of delubrication (melting and evaporation) can be detected by the O_2 sensor with evaporation starting at ~270 °C and the later stages (decomposition) detected by the CO_2 sensor with a peak maximum at ~410 °C, by the use of which the process can be monitored and controlled.

8.2 Effect of Process Parameters on Delubrication

- The process atmosphere composition, purity (presence of moisture), presence of admixed graphite, holding time at 450 °C, change in the flow rate above the nominal level (4 L/min), increase in density to 7.3 g/cc and increase in process temperature above 450 °C, all have minimum effect on the efficiency of lubricant removal.
- The increase in the heating rate shifts the delubrication process towards higher temperatures in which case higher temperatures (~500 °C) would be necessary for complete lubricant removal.
- At higher temperatures and higher heating rates, decreasing the flow rate below nominal settings results in slight oxidation indicated by discoloration of the specimen. When the flow rates are significantly reduced to almost static conditions and the processing temperature was reduced to 400 °C or below, deposition of decomposition products on the sample surfaces was observed.

8.3 Changes in Surface Chemistry during Delubrication and their Effect on Sintering

- Delubrication performed at 450 °C in dry N_2 preserves the surface chemistry of the original powder, and the compacts upon further sintering exhibit optimum properties.
- Delubrication at 900 °C results in the growth of thermodynamically stable Cr-Mn spinel oxides at the expense of the easily reducible Fe-oxide layer and consequently upon further sintering contributes to inferior mechanical properties.
- Sintering after delubrication in air at 450 °C results in inferior mechanical properties. This is due to the significant oxidation, contributing to a five-fold increase in the oxygen content of the compacts during delubrication, the reduction of which results in a significant carbon-loss and consequently inferior properties.
- Delubrication at 300 °C results in insufficient lubricant removal contributing to inferior mechanical properties after sintering due to the presence of regions with lower degree of necking where the residual lubricant would have been present.

8.4 Effect of Active Constituents in the Atmosphere on the Sintering of Chromium-Alloyed PM Steels

Carbon Monoxide

- Atmospheres containing carbon monoxide as the only active constituent exhibit high oxidation potential for chromium-alloyed PM steels during the heating stage of the sintering cycle until ~1000 °C for carbon monoxide concentrations above ~1 vol.%, with oxidation proportional to the carbon monoxide content in the atmosphere.
- Carburization was also observed and follows a similar trend with carbon concentration.
- Carbon dissolution in the matrix was observed already at 1000 °C, indicating partial reduction or transformation of the previously existing continuous Fe-oxide making it discontinuous.

Hydrogen

- Reduction of the surface iron oxide takes place at temperatures below 650 °C in hydrogen-containing atmospheres where the 'peak' temperature corresponding to the reduction decreases with an increase in the concentration of hydrogen.
- In these atmospheres reduction of Fe-rich/spinel oxides and internal oxides occurs above 800 and 1200 °C, respectively.
- Graphite is the dominant reducing agent even in hydrogen-rich atmospheres.

Carbon Monoxide and Hydrogen

- The compacts sintered in atmospheres with both hydrogen and carbon monoxide as the active components exhibit higher carburization and lower oxidation/better reduction compared to atmospheres with carbon monoxide as the only active constituent.
- This also implies an improved buffering capacity with hydrogen addition.
- Presence of additional propane has no significant influence on the carburization, but improves the reducing ability of the atmospheres in the range of concentrations and sintering temperatures examined.

Lean Sintering Atmospheres

- Based on thermodynamic calculations, three different atmosphere compositions were proposed for experimental studies containing carbon monoxide, hydrogen, propane and oxygen.
- Experimental studies have shown that the proposed atmospheres provide carburization during sintering process with carburization being proportional to the carbon monoxide and hydrogen concentrations and inversely proportional to the cooling rate and sintering temperature.
- It is demonstrated that the proposed atmospheres are promising candidates for the sintering of chromium-alloyed PM steels.

9 SUGGESTIONS FOR FUTURE WORK

9.1 Delubrication

- Development of additives that can promote clean delubrication
- Studying the effect of delubrication on the mechanical properties of the sintered compacts at an industrial scale
- Study of the effect of the risk of delubrication at different temperatures and process-gas flow rates, i.e., the effect of extent of lubricant evaporation and decomposition, on the furnace contamination in an industrial sintering process
- Evaluation of parameters such as furnace load and part geometry on the delubrication process in industrial furnaces

9.2 Sintering

- Establishment of the mechanism of graphite dissolution during the heating stage and the effect of pore "microclimate" on the dissolution process and its rate
- Studying the temperature ranges for direct and indirect carbothermal reduction with regard to the alloy system, carbon source and their relation to the sintering atmosphere
- Develop a thermodynamic and kinetic model for carburization/decarburization and oxidation/reduction for lean atmospheres containing CO, H_2 and hydrocarbons with respect to the concentration of the active gas constituents and the temperature profile
- Application of the proposed lean atmospheres in industrial furnaces along with the analysis of mechanical performance of the sintered compacts

10 ACKNOWLEDGEMENTS

11 REFERENCES

[1] R. M. German, *Powder Metallurgy of Iron and Steel*. Wiley Interscience, 1998.

[2] M. Hull, "Astaloy CrM: new generation powder from Höganäs," *Powder Metall. 1998*, vol. 41, no. 4, pp. 232–233, 1998.

[3] "Practical problems during sintering of ferrous parts," *Metal Powder Report*, pp. 26–30, 1994.

[4] "Shaping and Consolidation Technologies," in *Powder Metal Technologies and Applications, ASM Handbook Vol.7*, ASM International, 1998, pp. 453–467.

[5] J. J. Thomas, P. R. Daniel, and L. F. Stephen, "Delubrication Byproduct Reactions using Various Assist Systems of Powdered Metal Compacts," in *Advances in Powder Metallurgy and Particulate Materials*, 1996, pp. Vol.3, 10–17 to 10–26.

[6] S. L. Feldbauer, "Gassing up to get the right atmosphere," *Met. Powder Rep.*, vol. 62, no. 5, pp. 14–19, May 2007.

[7] G. White and H. Nayar, "Monitoring of the Delubrication Process Under Production," *Adv. Powder Metall. Part. Mater.*, vol. 3, pp. 10–27 to 10–40, 1996.

[8] M. M. Baum, R. M. Becker, A. M. Lappas, J. A. Moss, D. Apelian, D. Saha, and V. A. Kapinus, "Lubricant Pyrolysis during Sintering of Powder Metallurgy Compacts," *Metall. Mater. Trans. B*, vol. 35B, no. April, pp. 381–392, 2004.

[9] P. Quadbeck, B. Schreyer, A. Strauß, T. Weißgärber, and B. Kieback, "In-Situ Monitoring of Gas Atmospheres During Debinding and Sintering of PM Steel Components," *PM2010 World Congr.*, vol. 2, pp. 239–245, 2010.

[10] H. Karlsson, L. Nyborg, and S. Berg, "Surface chemical analysis of prealloyed water atomised steel powder," *Powder Metall.*, vol. 48, no. 1, pp. 51–58, Mar. 2005.

[11] D. Chasoglou, E. Hryha, M. Norell, and L. Nyborg, "Characterization of surface oxides on water-atomized steel powder by XPS/AES depth profiling and nano-scale lateral surface analysis," *Appl. Surf. Sci.*, vol. 268, pp. 496–506, Mar. 2013.

[12] P. Quadbeck, B. Schreyer, A. Strauß, T. Weißgärber, and B. Kieback, "In-Situ Monitoring of Gas Atmospheres During Debinding and Sintering of PM Steel Components," *PM World Congr.*, vol. 2, pp. 239–245, 2010.

[13] P. Ramakrishnan, "History of Powder Metallurgy," *Indian J. Hist. Sci.*, vol. 18, no. 1, pp. 109–114, 1983.

[14] S. Werner and W. Klaus-Peter, *Powder Metallurgy Processing and Materials*. European Powder Metallurgy Association, 1997.

[15] EPMA, "Powder Metallurgy — Intrinsically Sustainable." [Online]. Available: www.epma.com.

[16] I. Cremer, "Review of European PM Market," in *PM2012 World Congress*, 2012.

[17] M. Bulger, "State of the PM industry in North America," in *PM2012 World Congress*, 2012.

[18] H. Karlsson, L. Nyborg, and S. Berg, "Powder, Surface Chemical Analysis of Prealloyed Water-atomised Steel," *Powder Metall.*, vol. 48, no. 1, pp. 51–58, 2005.

[19] D. Chasoglou, "Surface Chemical Characteristics of Chromium-alloyed Steel Powder and Role of Process Parameters during Sintering," PhD Thesis, Chalmers University of Technology, 2012.

[20] E. Hryha, C. Gierl, L. Nyborg, H. Danninger, and E. Dudrova, "Surface composition of the steel powders pre-alloyed with manganese," *Appl. Surf. Sci.*, vol. 256, no. 12, pp. 3946–3961, Apr. 2010.

[21] O. Bergman, "Key Aspects of Sintering Powder Metallurgy Steel Prealloyed with Chromium and Manganese," PhD Thesis, Chalmers University of Technology, 2011.

[22] S. Karamchedu, S. Hatami, L. Nyborg, and M. Andersson, "Sinter-Hardening Response of Sintered Steel Based on Astaloy Mo and Its Diffusion Bonded Derivatives," *Powder Metall. Prog.*, vol. 14, no. 2, pp. 93–98, 2014.

[23] "Sintering of Iron based Materials," in *Höganäs Handbook 9*, Höganäs AB, Sweden.

[24] P. Knutsson, K. Olsson, M. Larsson, and M. Dahlberg, "Solutions for High Density PM Components," in *Proceedings of PM 2010 World Congress, Florence*, 2010, p. Vol.1.

[25] U. Engström, N. Solimanjad, K. Backer, R. Menzel, and P. Rauch, "An Integrated Approach to Optimize the Interaction of Powder Concepts, Tooling and Compaction Aspects in PM Component Manufacturing," in *PM2010 World Congress*, 2010.

[26] D. Milligan, P. Hofecker, U. Engström, M. Larsson, and S. Berg, "A comparison of methods for reaching high green densities using elevated temperatures," in *International Conference on Powder Metallurgy and Particulate Materials*, 2004.

[27] K. Takashi, O. Tomoshige, and O. Yukiko, "Analysis of Dewaxing Behavior of Iron Powder Compacts Based on a Direct Observation of Decomposing Lubricant During Sintering in a Furnace," *JFE Tech. Rep.*, vol. 16, no. 16, pp. 83–88, 2011.

[28] J. Dwyer, H. Nayar, W. Gerristead, and B. Wasiczko, "Comparative studies of P/M lubricants under different atmospheres using TGA techniques," in *Advances in Powder Metallurgy and Particulate Materials*, 1992, vol. 3, pp. 183–192.

[29] K. Hallhagen, O. Thornblad, and H. Storstršm, "The Influence of Lubricants in Powder Compaction," *Met. Powder Rep.*, vol. 53, no. 2, p. 42, 1998.

[30] A. I. Lawrence, S. H. Luk, and J. A. Hamill, "A Performance Comparison of Current P/M Lubricants and Routes to Improvement," in *International Conference on Powder Metallurgy & Particulate materials*, 1997, pp. 1–22.

[31] S. St-laurent, O. Wang, R. Guo, K. Zhang, and A. Cao, "Achieving High Density By Single Compaction Of Steel Powder Premixes," in *PM 2010 World Congress*.

[32] E. Hjortsberg, L. Nyborg, and H. Vidarsson, "Microscopic characterisation of topography and lubricant distribution on surface of powder compacts," *Powder Metall.*, vol. 48, no. 4, pp. 345–353, Dec. 2005.

[33] Z. A. Munir, "Analytical treatment of the role of surface oxide layers in the sintering of metals," *J. Mater. Sci.*, vol. 14, no. 11, pp. 2733–2740, Nov. 1979.

[34] Z. A. Munir, "Surface oxides and sintering of metals," *Powder Metall.*, vol. 24, no. 4, pp. 177–180, 1981.

[35] S. Kremel, C. Raab, and H. Danninger, "Contact Formation and Carbon Dissolution during Sintering of Steels prepared from Astaloy CrM," in *Euro PM 2001*, 2001, pp. Vol.1, 52–57.

[36] R. Frykholm, O. Bergman, and H. Ab, "Chromium pre-alloyed PM steels suitable for high performance applications," in *PMTEC2005*, 2005.

[37] S. Berg, "P/M Steel Suitable for Sinterhardening in Respect of Cost and Performance," in *Advances in Powder Metallurgy and Particulate Materials*, 2001, pp. 5–18 (4).

[38] E. Hryha, E. Dudrova, and S. Bengtsson, "Influence of Powder Properties on Compressibility of Pre-Alloyed Atomized Powders," *Powder Metall.*, vol. 5, p. Vol–3, pp.3 to 8, 2007.

[39] C. Oikonomou, E. Hryha, L. Nyborg, and Å. Ahlin, "Effect of Powder Properties on the Compressibility of Water-Atomized Iron and Low-Alloyed Steel Grades," in *Proceedings of Euro PM2013*, 2013, pp. 205–212.

[40] J. M. Torralba, R. De Oro, and M. Campos, "From Sintered Iron to High Performance PM Steels," *Mater. Sci. Forum*, vol. 672, pp. 3–11, Jan. 2011.

[41] T. Minegishi, S. Unami, O. Furukimi, and K. Komamura, "Mechanical Properties of Sintered Compacts made from Low-Oxygen Ct-Alloyed Steel Powder," in *Advances in Powder Metallurgy & Particulate Materials*, 1992, pp. Vol.5, pp53.

[42] S. Takajo, N. Yamato, Y. Marda, and Y. Morioka, "Cr Containing Steel Powder made by Modified Composite-Type Alloying for Wear Resistant PM Parts of Higher Strength," in *Metal Powder Report*, 1987, p. Vol 42, Pp.292.

[43] E. Hryha, E. Dudrova, and L. Nyborg, "Critical Aspects of Alloying of Sintered Steels with Manganese," *Metall. Mater. Trans. A*, vol. 41, no. 11, pp. 2880–2897, Jul. 2010.

[44] P. Ortiz and F. Castro, "Thermodynamic and experimental study of role of sintering atmospheres and graphite additions on oxide reduction in Astaloy CrM powder compacts," *Powder Metall.*, vol. 47, no. 3, pp. 291–298, Sep. 2004.

[45] Y. Y, "Thermodynamic and Kinetic Behaviours of Astaloy CrM," in *Proceedings of 2000 Powder Metallurgy World Congress*, 2000.

[46] E. C. Bain, "The Effect of Alloying Elements on Steels," Cleveland, 1939.

[47] L. Wimbert, K. Dollmeier, V. Kruzhanov, and R. Lindenau, "Advanced Lubricants – A Complex Challenge for Powder Metallurgy : Density , Lubricity , Environment," in *Advanced Lubricants- A Complex Challenge for Powder Metallurgy-Density, Lubricity, Environment*, 2010.

[48] M. Ward, "Influence of lubricants on dimensional changes and mechanical properties of sintered ferrous compacts," *Powder Metall.*, no. 4, pp. 193–200, 1979.

[49] J. N. Auborn and J. S. Choo, "Effect of Chemistry and Compact Density on the Decomposition of P/M Lubricants," *Adv. Powder Metall. Part. Mater.*, vol. 3, pp. 103–106, 1994.

[50] S. L. Feldbauer, "Advances in Powder Metal Sintering Technology," *Ind. Heat.*, vol. 73, no. 12, p. 51, 2006.

[51] B. I. Bondarenko, I. V Voloshin, Y. A. Voloshina, V. D. Artem'ev, L. E. Rubinchik, and S. G. Ruzhanskii, "Oven Operation in Sintering Powder Components Plasticized with Zinc Stearate," *Poroshkovaya Metall.*, no. 5, pp. 461–464, 1993.

[52] M. Renowden and P. Pourtalet, "Experimental Studies on Lubricant Removal," *Met. Powder Rep.*, vol. 1990, no. 9, pp. 625–628.

[53] A. Taskinen and M. Tikkanen, "A new method for studies of lubricant decomposition phenomena during sintering," *Scand. J. Metall.*, vol. 10, pp. 35–38, 1981.

[54] G. F. Bocchini, "Influence of Controlled Atmospheres on the Proper Sintering of Carbon Steels," *Powder Metall. Prog.*, vol. 4, no. 1, pp. 1–34, 2004.

[55] N. Harb and W. George, "Indication of Complete Delubing," *Adv. Powder Metall. Part. Mater.*, vol. 1, pp. 3–11 to 3–18, 1995.

[56] T. Pieczonka, K. J. Kurzyd, J. Mizera, and J. Kazior, "Acrawax C Removal from Aluminium-based Compacts," in *World PM 2012*, 2012.

[57] D. Saha and D. Apelian, "Control of de-lubrication utilizing a logistic function based emperical model," in *Proceedings of 2001 International Conference on Powder Metallurgy and Particulate Materials*, 2001, pp. Vol.5, 103–112.

[58] D. Saha, "De-Lubrication During Sintering of P/M compacts: Operative Mechanism and Process Control Strategy," MSc Thesis, Worcester Polytechnic Institute.

[59] A. Gateaud, "Physical and Chemical Mechanisms of Lubricant Removal During Stage I of the Sintering Process," MSc Thesis, Worcester Polytechnic Institute, 2006.

[60] R. M. German, "Thermal extraction of binders and lubricants in sintering," in *Advances in Powder Metallurgy and Particulate Materials*, pp. 10–13 to 10–16.

[61] "Designing for P/M- Processing," in *Handbook, Höganäs*, .

[62] A. Taskinen, M. Tikkanen, and G. Bockstiegel, "Carbon deposition on PM parts during the delubrication process," *Scand. J. Metall.*, vol. 10, pp. 55–62, 1981.

[63] S. Yousefli, "Analyzing the Causes of Blistering in Sintered Iron Parts: A Case Study in the Iran Powder Metallurgy Complex," *Powder Metall. Prog.*, vol. 11, no. 1, pp. 149–152, 2011.

[64] S. Andersson and M. A. Ahlqvist, "TGA-FTIR Evaluation of the Dewaxing Process," in *1998 PM World Congress*, 1998, pp. Vol.2, 261–265.

[65] J. McGraw, M. Koczak, and A. Kao, "Investigatin in the Delubrication of P/M Compacts," *Int. J. Powder Metall. Powder Technol.*, vol. 14, no. 4, p. 277 to 288, 1978.

[66] C. F. Legzdins, I. V Samarasekera, and T. Troczynski, "Experimental Studies of Zinc Stearate Delubrication in High Temperature Sintering of Ferrous Compacts," in *PM World Congress*, 1998, pp. Vol.2, 266–271.

[67] G. A. Poskrebyshev, M. M. Baum, J. A. Moss, and D. Apelian, "Catalytic effect of Fe/C powder on the formation of gas-phase products of vacuum pyrolysis of N,N′-ethylenebisstearamide," *Appl. Catal. A Gen.*, vol. 327, no. 1, pp. 52–65, Jul. 2007.

[68] M. Phillips and P. Pourtalet, "Understanding parameters for removal of lubricants from P/M tool steels and stainless steels to improve quality," *Ind. Heat.*, no. 5, pp. 37–43, 1993.

[69] K. H. Moyer, "How Argon Can Assist in Providing Clean Burn-Off of Lubricants and Binders." Advances in Powder Metallurgy and Particulate Materials, pp. 5–33 to 41, 2000.

[70] T. Holm, A. Malas, and S. Wiberg, "Furnace Atmospheres No.8- Sintering of steels," *Linde Gas*, no. 8.

[71] R. Andersson, H. Torsten, and S. Wiberg, "Linde Gas- Furnace Atmospheres No .2 : Neutral Hardening and Annealing," *Linde Gas*, no. 2.

[72] H. Danninger, C. Gierl, S. Kremel, G. Leitner, and Y. Yu, "Degassing and Deoxidation Processes During Sintering of Unalloyed and Alloyed PM Steels," *Powder Metall. Prog.*, vol. 2, no. 3, pp. 125–140, 2002.

[73] H. Danninger and C. Gierl, "Processes in PM steel compacts during the initial stages of sintering," *Mater. Chem. Phys.*, vol. 67, no. 1–3, pp. 49–55, Jan. 2001.

[74] E. Hryha, "Study of Reduction/Oxidation Processes in Cr-Mo Prealloyed Steels During Sintering by Continuous Atmosphere Monitoring," *Powder Metall. Prog.*, vol. 7, no. 4, pp. 181–197, 2007.

[75] M. Hrubovčáková and E. Dudrová, "Influence of the Purity of the Sintering Atmosphere on the Reduction of Oxides During Sintering of Fe-Cr-Mo Steels," *Powder Metall. Prog.*, vol. 10, no. 2, pp. 71–80, 2010.

[76] S. L. Elder, "Monitoring polymer burnout at the macroscale," *Powder Metall.*, vol. 47, no. 4, pp. 302–303, 2004.

[77] R. Speaker, R. Oesterreich, S. Kazi, and J. Buonassisi, "Sintering Atmosphere Analysis: Selection and use of Analyzers to monitor and control Sintering Atmospheres," in *Advances in Powder Metallurgy & Particulate Materials*, 2003, pp. 5–16 to 5–31.

[78] E. Hryha, L. Nyborg, a Malas, S. Wiberg, and S. Berg, "Carbon control in PM sintering: industrial applications and experience," *Powder Metall.*, vol. 56, no. 1, pp. 5–10, Feb. 2013.

[79] G. F. Bocchini, R. Cesari, M. R. Pinasco, and E. Stagno, "Sintering of Carbon Steels: Controlled Atmospheres, Equipment, Practical Results," *Mater. Sci. Forum*, vol. 299–300, pp. 224–248, 1999.

[80] H. Karlsson, L. Nyborg, S. Berg, and Y. Yu, "Surface Product Formation on Chromium Alloyed Steel Powder Particles," in *Euro PM 2001*, 2001, pp. Vol.1, pp.22–27.

[81] D. Chasoglou, E. Hryha, and L. Nyborg, "Effect of Sintering Atmosphere on the Transformation of Surface Oxides During the Sintering of Chromium Alloyed Steel," *Powder Metall. Prog.*, vol. 9, no. 3, pp. 141–155, 2009.

[82] D. Chasoglou, E. Hryha, and L. Nyborg, "Methodology for Evaluating the Oxide Distribution in Water Atomized Steel Powder," in *Euro PM 2009*, 2009, pp. Vol.2, pp.181–186.

[83] P. G. Mukunda, "Carbon absorption by iron during sintering of iron-graphite," *Powder Metall.*, vol. 27, no. 2, pp. 89–92, 1984.

[84] M. Eudier, "Role of atmosphere in sintering of copper steels," *Powder Metall.*, vol. 24, no. 3, pp. 151–154, 1981.

[85] E. Hryha, L. Nyborg, and L. Alzati, "Effect of Carbon Source on Oxide Reduction in Cr-Prealloyed PM Steels," *Proc. 2012 Powder Metall. World Congr. Exhib. Japan Powder Metall. Assoc. Japan Soc. Powder Powder Metall.*, no. 16A-T9–11, ISBN:978–4–9900214–9–8, 2012.

[86] E. Hryha, L. Nyborg, and L. Alizati, "Dissolution of Carbon in Cr-Prealloyed PM Steels: Effect of Carbon Source," *Powder Metall.*, vol. 58, no. 1, pp. 7–11, 2015.

[87] E. Hryha and L. Nyborg, "Efficiency of different carbon sources during sintering of Cr-prealloyed PM steels: Graphene, Graphite or carbon black," *Proc. PM2014 World Congr.*, 2014.

[88] H. Danninger, G. Frauendienst, K.-D. Streb, and R. Ratzi, "Dissolution of different graphite grades during sintering of PM steels," *Mater. Chem. Phys.*, vol. 67, no. 1–3, pp. 72–77, Jan. 2001.

[89] A. Simchi, H. Danninger, and C. Gierl, "Electrical conductivity and microstructure of sintered ferrous materials: iron–graphite compacts," *Powder Metall.*, vol. 44, no. 2, pp. 148–156, 2001.

[90] Y. K. Rao, "The Kinetics of Reduction of Hematite by Carbon," *Metall. Trans.*, vol. 2, no. May, pp. 1439–1447, 1971.

[91] N. S. Srinivasan and A. K. Lahiri, "Studies on the Reduction of Hematite by Carbon of iron I oxides E," vol. 8, no. March, pp. 175–178, 1977.

[92] M. C. Abraham and A. Ghosh, "Kinetics of Reduction of Iron Oxides and Ores by Carbon," 1973.

[93] E. Hryha and L. Nyborg, "Changes in oxide chemistry during consolidation of Cr/Mn water atomized steel powder," *Powder Metall. Prog.*, vol. 11, no. 1, pp. 42–50, 2011.

[94] S. Karamchedu, E. Hryha, and L. Nyborg, "Changes in the surface chemistry of chromium-alloyed powder metallurgical steel during delubrication and their impact on sintering," *J. Mater. Process. Technol.*, vol. 223, no. September, pp. 171–185, Sep. 2015.

[95] E. Hryha and L. Nyborg, "Oxide Transformation in Cr-Mn-Prealloyed Sintered Steels: Thermodynamic and Kinetic Aspects," *Metall. Mater. Trans. A*, vol. 45, no. 4, pp. 1736–1747 (print), 1543–1940 (online), 2014.

[96] E. Hryha and L. Nyborg, "Oxide Transformation During Sintering of Cr and Mn Prealloyed Water Atomized Steel Powder," in *Euro PM 2011*, 2011.

[97] O. Bergman, "Influence of Oxygen Partial Pressure in Sintering Atmosphere on Properties of Cr-Mo Prealloyed Powder Metallurgy Steel," *Powder Metall.*, vol. 50, no. 3, pp. 243–249, 2007.

[98] D. Chasoglou, E. Hryha, and L. Nyborg, "Effect of process parameters on surface oxides on chromium-alloyed steel powder during sintering," *Mater. Chem. Phys.*, vol. 138, pp. 405–415, 2013.

[99] E. Hryha, E. Dudrova, and L. Nyborg, "On-line control of processing atmospheres for proper sintering of oxidation-sensitive PM steels," *J. Mater. Process. Technol.*, vol. 212, no. 4, pp. 977–987, Apr. 2012.

[100] E. Hryha and L. Nyborg, "Oxide Transformation During Sintering Of Prealloyed Water Atomized Steel Powder," *Proc. PM 2010 World Congr.*, vol. 2, pp. 268–275, 2010.

[101] O. Bergman, K. Frisk, and L. Nyborg, "Analysis of Oxide Reduction during Sintering of Cr-alloyed Steel Powder through Photoacoustic Spectroscopy Measurements," *Proc. Euro PM 2009*, vol. 3, pp. 239–244, 2009.

[102] M. Dlapka, C. Gierl, H. Danninger, and S. Bengtsson, "Nitrogen Pickup During Sintering and Subsequent Cooling of Chromium Alloyed PM Steels," in *Proceedings of Euro PM2010, Vol.2*, 2010, pp. 13–20.

[103] O. Bergman and L. Nyborg, "Evaluation of Sintered Properties of PM Steels based on Cr and Cr-Mn Prealloyed Steel Powders," *Powder Metall. Prog.*, vol. 10, no. 1, pp. 1–19, 2010.

[104] O. Bergman, B. Lindqvist, and S. Bengtsson, "Influence of Sintering Parameters on the Mechanical Performance of PM Steels Pre-Alloyed with Chromium," *Mater. Sci. Forum*, vol. 534–536, pp. 545–548, 2007.

[105] H. J. Grabke, "Thermodynamics, mechanisms and kinetics of metal dusting," *Mater. Corros.*, vol. 49, no. 5, pp. 303–308, May 1998.

[106] P. Ortiz and F. Castro, "Influence of Carbon Activity and Oxygen Potential of Sintering Atmospheres on the Microstructural Characteristics of Low Alloy P/M Steels," *Mater. Sci. Forum*, vol. 426–432, pp. 4337–4342, 2003.

[107] L. Sproge and J. Ågren, "Experimental and theoretical studies of gas consumption in the gas carburizing process," *J. Heat Treat.*, vol. 6, no. 1, pp. 9–19, Mar. 1988.

[108] A. Costa e Silva, J. Ågren, M. T. Clavaguera-Mora, D. Djurovic, T. Gomez-Acebo, B.-J. Lee, Z.-K. Liu, P. Miodownik, and H. J. Seifert, "Applications of computational thermodynamics — the extension from phase equilibrium to phase transformations and other properties," *Calphad*, vol. 31, no. 1, pp. 53–74, Mar. 2007.

[109] H. S. Adams and S. M. Nayar, "Sintering Carbon Steel Under Atmospheres with Lowered Carbon Monoxide," *Prog. Powder Metall.*, 1986.

[110] B. Lindqvist and K. Kanno, "Considerations When Sintering Oxidation Sensitive PM Steels," in *Proceedings of World PM Congress 2002*, 2002, p. 13.278 , 13.290.

[111] O. Karabelchtchikova, "Fundamentals of Mass Transfer in Gas Carburizing," PhD Thesis, Worcester Polytechnic Institute, Worchester, Massachusetts, U.S. November, 2007.

[112] S. Karamchedu, Eduard Hryha, and L. Nyborg, "Lean atmospheres for sintering of chromium alloyed powder metallurgy steels," in press, Dresden, 2014.

[113] J. M. D. L. F. Ortiz, "High Performance Powder Metallurgy Parts by Surface and Microstructure Tailoring," 2007.

[114] B. Maroli, S. Berg, P. Thorne, and U. Engström, "Sinter-hardening and heat treatment of materials based on Astaloy CrM," *Adv. Powder Metall. Part. Mater.*, no. 5, p. 149, 2003.

[115] S. Bengtsson, T. Marcu, and A. Klekovkin, "Carburizing of Low-Alloyed Chromium Materials – An Overview," *Adv. Powder Metall. Part. Mater.*, pp. 155–156, 2008.

[116] L. Nyborg, S. Hatami, and S. Bengtsson, "Simulation of Mechanical Properties of Chromium Alloyed Sintered Steel," *Adv. Powder Metall. Part. Mater.*, vol. 1, no. 1, pp. 1–10, 2008.

[117] P. Beiss, "Sintering atmospheres for PM steels," in *Höganäs Chair in Powder Metallurgy Workshop " Sintering Atmospheres."*

[118] S. B. Francisco Castro, Angela Veiga, Frank Baumgaetner, Johannes Heyde, Stefano Saccarola, "Endogas Sintering of a Cr-containing PM steel," *Adv. Powder Metall. Part. Mater.*, pp. 07–46, 2012.

[119] P. R. Wilyman, "Sintering with nitrogen based atmospheres," *Powder Metall.*, vol. 28, no. 2, pp. 85–89, 1985.

[120] S. Ahonen, C. Laumen, and S. Wiberg, "New Method of Controlling the Carbon Content of High Chromium Alloyed Powders during High Temperature Sintering," *Mater. Sci. Forum*, vol. 591–593, pp. 300–307, 2008.

[121] J. Moulder, W. Stickle, P. Sobol, and K. Bomben, *Handbook of X-ray Photoelectron Spectroscopy*. Eden Prairie: Perkin-Elmer Corp, 1992.

[122] J. Lumsden, "X-ray Photoelectron Spectroscopy," in *ASM Handbook,* ASM International, 1986, pp. 568–580.

[123] G. Goldstein, D. Newbury, P. Echlin, D. Joy, C. FIori, and E. Lifshin, *Scanning electron microscopy and microanalysis*. New York: Plenum Press, 1981.